Research article

Comprehensive analysis of shared risk genes and immunity-metabolisms between non-alcoholic fatty liver disease and atherosclerosis via bulk and single-cell transcriptome analyses

Qian Hu [a,b,1], Yunfang Luo [c,d,1], Hao He [e], Hua Chen [f,**], Di Liao [c,d,*]

[a] Center for Medical Genetics, School of Life Sciences, Central South University, Changsha, Hunan, China
[b] Key Laboratory of Medical Genetics of Hunan Province, Central South University, Changsha, Hunan, China
[c] Department of Neurology, Xiangya Hospital, Central South University, Changsha, Hunan, China
[d] National Clinical Research Center for Geriatric Disorders, Central South University, Changsha, Hunan, China
[e] Xiangya School of Medicine, Central South University, Changsha, Hunan, China
[f] Department of Neurosurgery, the First people's Hospital of Changde City, Changde, Hunan, China

ARTICLE INFO

Keywords:
Non-alcoholic fatty liver disease
Atherosclerosis
Bioinformatics
Shared risk genes
Landscape
Immune and metabolism dysregulation

ABSTRACT

Objective: and design: Considering the clinical link between non-alcoholic fatty liver disease (NAFLD) and atherosclerosis (AS), we performed bioinformatics analysis to uncover their pathogenic interrelationship.
Methods and results: Data from the U.S. National Health and Nutritional Examination Survey (NHANES) 1999–2018 were included. Among 4851 participants in NHANES, NAFLD was significantly associated with atherosclerotic cardiovascular disease risk (ASCVD risk) (OR = 2.32, 95%CI: 2.04–2.65, P < 0.0001). We conducted WGCNA analysis for NAFLD (GSE130970) and AS (GSE28829) and identified three modules positively related to NAFLD severity and two modules accelerating atherosclerosis plaque progression. 198 key-modules genes were obtained via overlapping these modules. Next, we mined the disease-controlled differentially expressed genes (DEGs) from NAFLD (GSE89632) and AS (GSE100927), respectively. The final common risk genes (*ACP5, TP53I3, RPS6KA1, TYMS, TREM2, CA12,* and *IFI27*) were defined by intersecting the upregulated DEGs with 198 genes and validated in new datasets (GSE48452 and GSE43292). Importantly, they showed good diagnostic ability for NAFLD and AS. Immune infiltration analysis showed both illnesses have dysregulated immunity. Analysis of single-cell sequencing datasets NAFLD (GSE179886) and AS (GSE159677) uncovered different abnormal expressions of seven common genes in different immune cells while highlighting metabolic disturbances including upregulation of fatty acid biosynthesis, downregulation of fatty acid degradation and elongation. *Conclusion:* We found 7 shared hub genes with good diagnostic ability and depicted the landscapes of immune and metabolism involved in NAFLD and AS. Our results provided a comprehensive

* Corresponding author. Department of Neurology, Xiangya Hospital, Central South University, 87 Xiangya Street, Changsha, Hunan 410008, China.
** Corresponding author.
E-mail addresses: huqian@sklmg.edu.cn (Q. Hu), 2521428591@qq.com (Y. Luo), 936483206@qq.com (H. Chen), liaodi1118@csu.edu.cn (D. Liao).
[1] These authors contributed equally to this work and shared the first authorship.

association between them and may contribute to developing potential intervention strategies for targeting both disorders based on these risk factors.

1. Introduction

With the aging of the global population, the incidence of non-alcoholic fatty liver diseases (NAFLD) has surged in recent decades [1]. Characterized by excessive fat build-up within hepatocytes in the lack of alcohol consumption and other known causes of liver disease [2], NAFLD has become the most prevalent chronic liver disease, with an overall prevalence of 25 % globally and this trend is ongoing [3]. It encompasses a spectrum of disorders including simple steatosis, non-alcoholic steatohepatitis (NASH), advanced
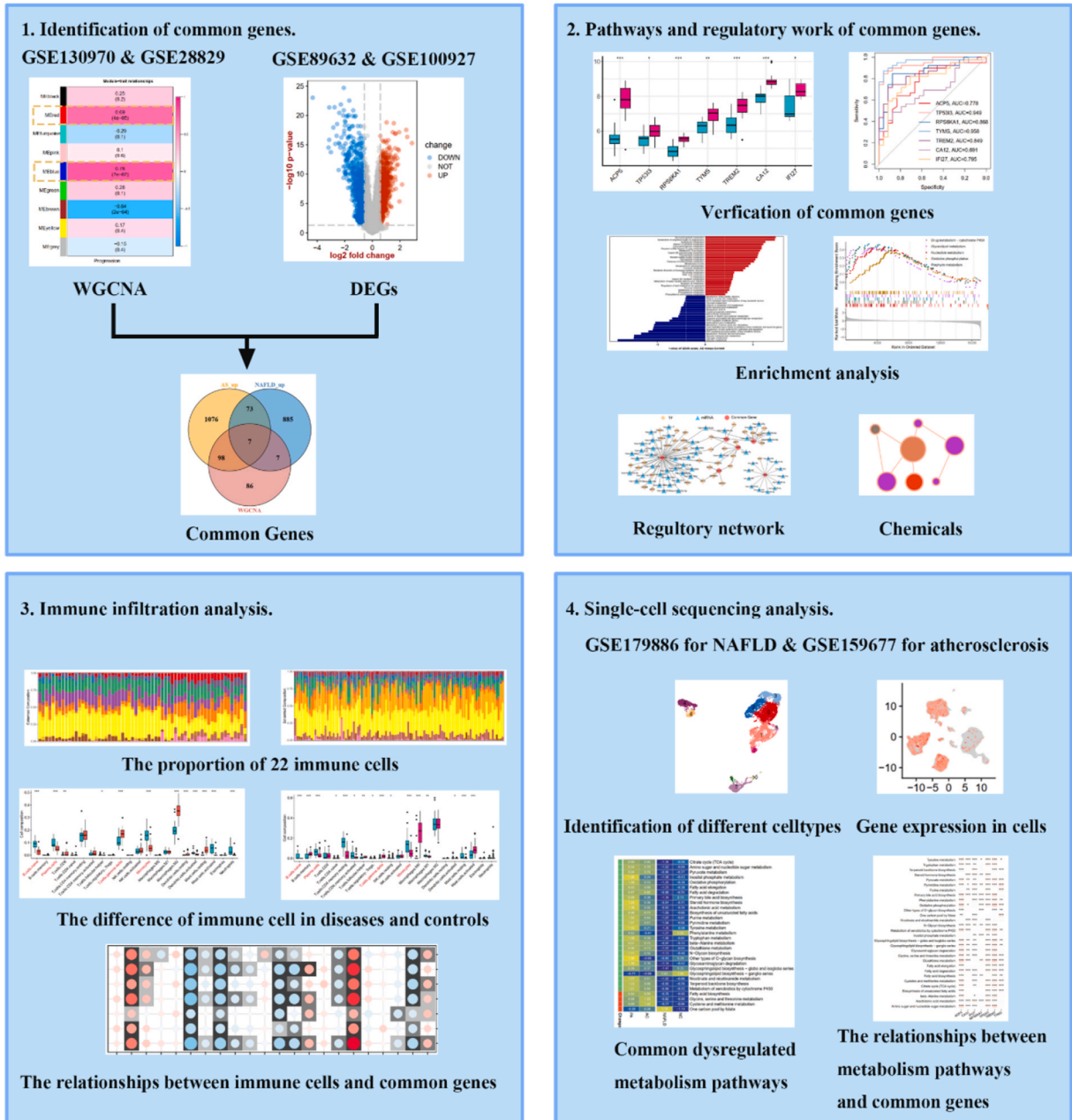

Fig. 1. Research technology flow chart of present work. WGCNA, weighted gene co-expression network analysis; DEGs, differentially expressed genes.

fibrosis, cirrhosis, etc [4]. As the liver is an important metabolic organ in the body, NAFLD is closely related to metabolic syndromes, such as insulin resistance, dyslipidemia, hypertension, and obesity [5,6]. Furthermore, growing evidence has shown that NAFLD is a risk factor for getting cardiovascular complications like atherosclerosis (AS) [7]. Recently, a new term for NAFLD has been proposed, known as metabolic associated fatty liver disease (MAFLD), reflecting the evolving understanding that MAFLD is purely a metabolic disorder [8,9]. Diagnosis of MAFLD is based on histological (biopsy), imaging, or blood biomarker evidence of hepatic steatosis, along with one of the following three criteria, namely obesity, type 2 diabetes mellitus (T2DM), or metabolic dysregulation [10].

Atherosclerosis (AS), characterized by lipid-rich plaques in the arterial wall, is a leading cause of mortality worldwide [11]. Atherosclerosis starts from pathologic lipid accumulation in the intima, which leads to bleeding and thrombosis, followed by fibroplasia and calcinosis over time, and gradual metamorphosis in the middle artery, resulting in narrowing of the vascular cavity and hardening of the artery wall [12]. Once the atherosclerotic plaque encroaches upon the lumen of the artery to block the blood flow, it will lead to tissue ischemia. Furthermore, atheromata can also induce ischemia by embolus detachment occluding the lumen. AS is the root cause of many cardiovascular diseases, such as ischemic stroke and coronary atherosclerotic heart disease [4,12]. Despite the improvements in prevention, enormous people die of acute complications of AS outside of the hospital.

Unfortunately, NAFLD and AS frequently co-occur. Indeed, clinical studies have found NAFLD to be an underestimated and independent risk factor for atherosclerotic cardiovascular diseases (ASCVD) even after adjustment for traditional risk factors covariates, such as dyslipidemia and dysglycemia [13]. Understandably, ectopic fat deposition in the liver and other tissues eventually exacerbated endothelial dysfunction and heightened systemic inflammatory tone, resulting in patients with NAFLD being predisposed to atherogenesis in the coronary, carotid, and peripheral arteries, which are liable to ischemic stroke and heart attacks [14]. Undoubtedly, ASCVD is the most common cause of death in patients with NAFLD. Existing common aberrant metabolic patterns, such as hyperlipidemia, insulin resistance, and hypertension, indicated NAFLD and AS may well be two sides of the same dysmetabolic coin [15].

Aside from disturbed metabolism, innate and adaptive immunity play a vital role in NAFLD and AS at different levels, and immune drift accelerates disease progression. Emerging evidence concerning inflammation involves NAFLD and becomes integral to the progression of the disease, particularly after progressing to the NASH stage [16]. Meanwhile, considering the immune system is crucial in driving AS-associated chronic inflammation, AS could also be called a chronic inflammatory disease. Extensive preclinical and clinical research have established that leukocytes including macrophages, T cells, and B cells with pro-inflammatory or regulatory functions could implicate the development and progression of NAFLD and AS [17–19].

However, the precise molecular mechanisms linking NAFLD and AS remain elusive. Identifying metabolic abnormalities and immune-modulating patterns will be crucial for the prevention and treatment of both now-ubiquitous diseases [16,17,20]. We herein analyzed GEO expression profiles of NAFLD and AS to unravel the shared risk genes, metabolism pathways, and immune microenvironment, which would inspire new ideas for the prediction and treatment of them. The article's research process is shown in Fig. 1.

2. Methods

2.1. NHANES

The data for statistical analysis was downloaded from the National Health and Nutrition Examination Survey (NHANES)(https://www.cdc.gov/nchs/index.htm). The NHANES is a research project aimed to assess the health and nutritional status of adults and children in the United States, combining interviews and physical examinations to provide vital health statistics. We screened 31,995 participants aged 40–79 from NHANES 1999 to 2018. 13728 non-Hispanic white participants were then included in the study. The ASCVD risk was assessed using the 10-year risk score for a first hard ASCVD event as outlined in the 2013 ACC/AHA guidelines [21]. The variables incorporated into the calculations encompassed age, sex, systolic blood pressure, total cholesterol, high-density lipoprotein cholesterol, diabetes mellitus, and current smoking status. Participants with a history of prior ASCVD, including self-reported instances of coronary heart disease, heart attack or myocardial infarction, angina pectoris, or stroke, were excluded from the analysis. An ASCVD risk ≥ 7.5 % was deemed indicative of a high risk of ASCVD. Participants were defined as NAFLD if their Fatty Liver Index (FLI) score [22] ≥ 60 or USFLI [23] ≥ 30 in the absence of hepatitis (positive hepatitis B virus surface antigen or positive hepatitis C virus antibody/RNA) and excessive alcohol consumption (>30 g/day for men or >20 g/day for women). After excluding those who had missing data of NAFLD or ASCVD risk, 4851 participants were included in our final analysis. The chi-square test or Student's t-test was performed to evaluate the differences between the non-exposure and exposure conditions on NAFLD. Logistic regression models

Table 1
The detailed descriptions of included GEO datasets in present work.

Accession	Platform	Type	Tissue sources	Sample
GSE130970	GPL16791	mRNA profile	liver	NAFLD:HC = 72:6
GSE89632	GPL14951	mRNA profile	liver	NAFLD:HC = 39:24
GSE48452	GPL11532	mRNA profile	liver	NAFLD:HC = 32:14
GSE28829	GPL570	mRNA profile	AS plaque	Advanced:Early = 16:13
GSE100927	GPL17077	mRNA profile	AS lesions and control arteries	AS plaque: Control = 69:35
GSE43292	GPL6244	mRNA profile	AS plaque	AS plaque: intact tissue = 32:32
GSE179886	GPL24676	sc-RNA sequencing	PBMCs	NAFLD: HC = 1:1
GSE159677	GPL18573	sc-RNA sequencing	AS plaque	AS core: proximal adjacent = 3:3

were performed to calculate odds ratios (ORs) for NAFLD and ASCVD.

2.2. GEO dataset download and process

We downloaded the original or processed gene expression profiles from the Gene Expression Omnibus (GEO) Dataset [24] by using the keywords "Nonalcoholic Fatty Liver Disease" or "atherosclerosis" to search NAFLD and atherosclerosis plaque gene expression profiles (https://www.ncbi.nlm.nih.gov/gds). Three NAFLD-related datasets (GSE130970, GSE89632, and GSE48452) and three atherosclerosis plaque-related datasets (GSE28829, GSE100927, and GSE43292) were finally included in our study. Besides, we also obtained two single-cell sequencing datasets (the GSE179886 dataset from peripheral blood mononuclear cells of NAFLD and the GSE159677 dataset for atherosclerosis plaque) from the GEO website. The detailed information was described in Table 1. The pre-processing of the dataset can be found in our previously published studies [25,26].

2.3. Weighted gene co-expression network analysis

To elucidate the genetic mechanisms in NAFLD and AS progression, the GSE130970 and GSE28829 datasets were used to construct a co-expression network by the WGCNA package in R [27]. Genes with the top 5000 median absolute deviations from the GSE130970 and GSE28829 datasets were extracted and clustered into different modules based on the scale-free topology (independence index R2 = 0.85) by using the pickSoftThreshold function and one-step network construction method. Pearson correlation analysis was conducted to estimate the association between disease phenotypes and genes. The modules with obvious significant correlation with the disease progression were identified.

2.4. Differentially expressed genes

We identified differentially expressed genes (DEG) between controls and diseases in the GSE89632 and GSE100927 datasets using the "limma" package [28] based on criteria of |log2fold change (FC)| > 0.58 and p-value <0.05. The common genes between NAFLD and AS were selected by overlapping the genes with the same trend, which were further intersected with the above module genes.

2.5. Function enrichment analysis

To investigate the biological function and pathway of common genes, Biological processes (BPs) of Gene Ontology (GO) and Kyoto Encyclopedia of Genes and Genomes (KEGG) were performed using the "clusterProfiler" package [29]. Moreover, We also used gene set enrichment analysis (GSEA) to identify potential disease pathways and gene set variation analysis (GSVA) to reveal the dysregulated metabolism processes with the "GSVA" R package [30].

2.6. Regulatory network and potential chemicals of common genes

The protein-protein interaction (PPI) networks and co-expression interaction of the common genes were constructed by GENE-MANIA software [31]. The upstream transcription factors (TFs) and microRNAs (miRNAs) of common genes were predicted by using the RegNetwork [32] database through the NetworkAnalyst website (https://www.networkanalyst.ca/NetworkAnalyst/) [33]. The potential chemicals targeting the common genes were searched from the Comparative Toxicogenomics Database (CTD) [34]. The regulatory network and interactions were visualized in Cytoscape software [35].

2.7. Validation of common genes in internal and external datasets

The levels of common genes expression were examined between illnesses and controls in GSE130970 and GSE89632 NAFLD datasets and GSE28829 and GSE100927 AS datasets. Further, we also recruited two external datasets (GSE48452 for NAFLD and GSE43292 for AS) to verify the shared genes expression levels. The diagnostic efficiency of the common genes in each dataset was visualized by using the ROC curve and assessed with the area under the curves (AUCs).

2.8. Immune cells infiltration analysis

CIBERSORTx [36] was adopted to estimate the cellular abundance and relative fractions of 22 subtypes of immune cells of NAFLD and AS in GSE89632 and GSE100927 datasets. The relationships between immune cells and shared genes were calculated by using the Pearson correlation method.

2.9. Single-cell sequencing analysis

GSE179886 dataset from peripheral blood mononuclear cells (PBMCs) of NAFLD and health control and GSE159677 dataset with the single-cell transcriptome of whole calcified atherosclerotic core (AC) plaques and partial patient-matched proximal adjacent (PA) carotid artery tissue were included to conduct single-cell sequencing analysis. We applied the "Seurat" package in R to group cells into appropriate clusters, with the resolution set to 0.3 after quality controls. The "SingleR" package was used to annotate the cell types of

the GSE179886 dataset, and for the atherosclerosis plaque, marker genes of different vascular cell types were applied for manually annotating the GSE159677 dataset cell types. The "scMetabolism" package was used to calculate the scores of the different metabolism-related pathways for both datasets [37]. The differences between diseases and controls were compared with the Wilcoxon test and the commonly dysregulated pathways were visualized by the "pheatmap" package. The relationships between common metabolism-related pathways and shared genes were calculated by using the Pearson correlation method.

2.10. Statistical analysis

R software (version R-4.1.0) was applied to perform all statistical analysis. The Wilcoxon test was used for statistical analysis between two groups. The relationships of genes with immune cells were constructed by using the Pearson method. P < 0.05 was considered to indicate statistical significance. The significance level is denoted as follows: *P < 0.05, **P < 0.01, and ***P < 0.001.

3. Results

3.1. The significant association between ASCVD and NAFLD

The baseline characteristics of 4851 participants and odds ratios for ASCVD and NAFLD were show n in Table 2. Compared with non-exposure conditions, the odds ratios (ORs) with 95 % confidence intervals (CIs) for exposure conditions between NAFLD and

Table 2
Baseline characteristics and odds ratio of participants by ASCVD risk levels.

Variable	ASCVD risk		P-value 1	OR (95 % CI)	P-value 2
	Low	High			
NAFLD			<0.0001		
No	1506(56.38)	800(35.74)		ref	ref
Yes	1155(43.62)	1390(64.26)		2.32(2.04,2.65)	<0.0001
Age	50.59(0.20)	64.82(0.23)	<0.0001	1.22(1.21,1.24)	<0.0001
Sex			<0.0001		
Male	1041(39.94)	1317(60.78)		ref	ref
Female	1620(60.06)	873(39.22)		0.43(0.38,0.49)	<0.0001
Education level			<0.0001		
Less Than 9th Grade	48(1.31)	146(4.61)		ref	ref
9-11th Grade	231(6.76)	254(9.78)		0.41(0.26,0.64)	<0.0001
High school graduate	597(21.42)	662(29.13)		0.39(0.25,0.61)	<0.0001
Some College	857(32.01)	625(30.13)		0.27(0.17,0.41)	<0.0001
College Graduate	927(38.51)	503(26.35)		0.19(0.12,0.31)	<0.0001
Marital status			<0.0001		
Married	1786(71.66)	1409(68.07)		ref	ref
Separated	59(1.72)	20(0.71)		0.43(0.23,0.82)	0.01
Never	169(5.80)	106(4.92)		0.89(0.64,1.24)	0.50
Divorced	422(14.49)	282(11.76)		0.85(0.71,1.03)	0.09
Widowed	83(2.55)	284(10.88)		4.50(3.40,5.96)	<0.0001
Living with partner	111(3.80)	68(3.67)		1.02(0.71,1.45)	0.93
Poverty	3.78(0.05)	3.26(0.05)	<0.0001	0.79(0.76,0.83)	<0.0001
BMI[a]	28.63(0.16)	29.68(0.18)	<0.0001	1.03(1.02,1.04)	<0.0001
Waist circumference (cm)	98.27(0.39)	105.23(0.39)	<0.0001	1.03(1.02,1.03)	<0.0001
Triglycerides(mg/dl)	125.76(1.78)	170.49(4.82)	<0.0001	1.00(1.00,1.00)	<0.0001
LDL[b]-cholesterol (mg/dl)	122.87(0.65)	122.49(1.18)	0.77	1.00(1.00,1.00)	0.77
HDL[b]-cholesterol (mg/dl)	57.43(0.38)	51.69(0.43)	<0.0001	0.98(0.97,0.98)	<0.0001
Total cholesterol (mg/dl)	205.58(0.81)	206.55(1.42)	0.53	1.00(1.00,1.00)	0.53
Smoke			<0.0001		
Never	822(39.54)	1375(55.16)		ref	ref
Former	882(37.56)	804(30.23)		1.73(1.52,1.98)	<0.0001
Now	486(22.90)	482(14.61)		2.19(1.83,2.61)	<0.0001
Hypertension			<0.0001		
No	1810(68.36)	754(35.47)		ref	ref
Yes	851(31.64)	1436(64.53)		3.93(3.39,4.57)	<0.0001
Cancer			<0.0001		
No	2404(90.54)	1697(79.13)		ref	ref
Yes	255(9.46)	491(20.87)		2.52(2.09,3.05)	<0.0001
DM[c]			<0.0001		
No	1056(49.44)	2067(78.04)		ref	ref
Borderline	471(20.51)	419(15.84)		2.04(1.72,2.42)	<0.0001
Yes	663(30.05)	175(6.12)		7.75(6.33,9.50)	<0.0001

[a] BMI: body mass index.
[b] LDL/HDL: low/high density lipoprotein.
[c] DM: diabetes mellitus.

ASCVD was 2.32 (2.04, 2.65), P < 0.0001. The results showed that NAFLD was significantly associated with a high risk of ASCVD, which indicates the significant links between ASCVD and NAFLD.

3.2. Identification of co-expression modules in AS and NAFLD

To construct the scale-free topology model, the soft thresholds 2 and 16 were selected to construct a co-expression network in GSE130970 and GSE28829 datasets, respectively (Fig. 2A and D, and Fig. S1). A total of 13 and 9 related co-expression modules were respectively merged with a threshold of 0.25 and a minimum gene size of 30 in the GSE130970 and GSE28829 datasets (Fig. 2B and E). Then, we calculated the Module-phenotypes relationship to detect the key modules related to the disease progression. For NAFLD, three modules (blue, turquoise, and pink) were relatively correlated with the severity of diseases, such as cytological ballooning grade,
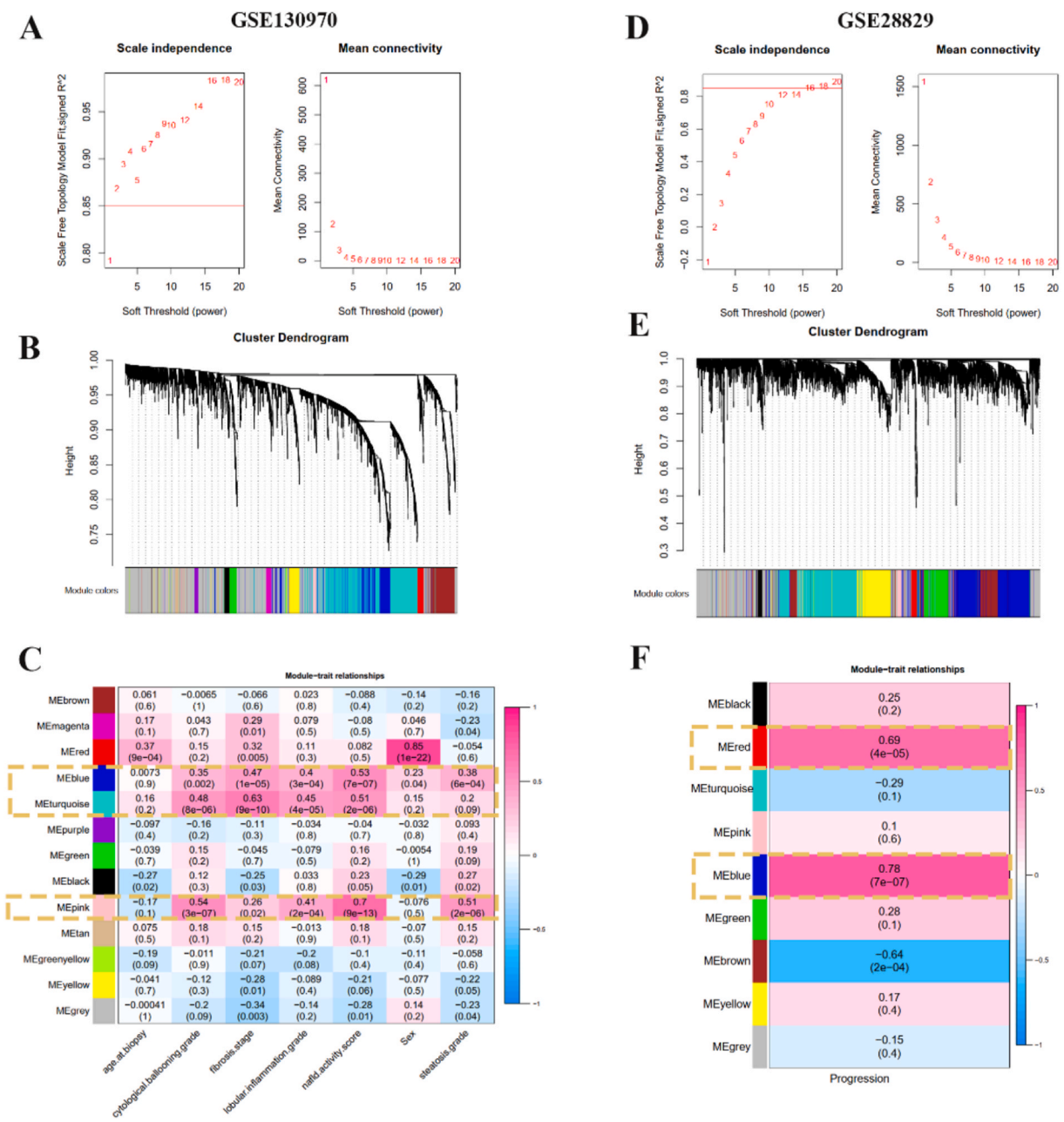
Fig. 2. Construction and identification of co-expression modules by WGCNA in GSE130970 and GSE28829 datasets. (A) and (D) Selecting the soft-threshold powers for constructing the scale-free topology network. (B) and (E) The cluster dendrogram of co-expression genes. (C) and (F) The module-trait relationships.

fibrosis grade, NAFLD activity score, and steatosis grade (Fig. 2C). Notably, these three modules demonstrated positive correlations with disease grading. Additionally, two modules (red and blue) that were positively correlated with the progression of AS from early to advanced plaque in the GSE28829 dataset were ultimately chosen (Fig. 2F).

3.3. The identification of 198 key-modules genes in AS and NAFLD

After merging the key modules correlated with each disease, a total of 1826 genes were identified for NAFLD and 1119 genes were identified for AS. Subsequently, these genes were compared to find the potentially shared risk genes for both disorders, resulting in the identification of 198 key-modules genes. The findings are illustrated in Fig. 3A. The BP of GO analysis showed that these 198 genes participated in immune regulation, such as positive modulation of cytokine production, T cell activation, and leukocyte migration (Fig. 3B). The KEGG results also indicate similar results revealing the involvement of immune-related pathways, such as the phagosomes, cytokine-cytokine-receptor interactions, and antigen processing and presentation (Fig. 3C).

3.4. Differentially expressed genes and functional enrichment analysis

We utilized the limma R to screen for DEGs between diseases and controls from NAFLD GSE89632 and AS GSE100927 datasets (Table S1 and Table S2). The principal component analysis revealed the distinguished distribution of diseases and controls (Fig. S2). In NAFLD, 972 down-regulated and 1429 up-regulated genes were identified (Fig. 4A) and their expression patterns were indicated by a heat map (Fig. 4B). After ranking DEGs by fold change, the GSEA enrichment analysis showed the metabolism-related pathways, such as glycerolipid metabolism and oxidative phosphorylation, were most enriched in NAFLD diseases when in comparison with the control group (Fig. 4C). In the AS dataset, 1985 DEGs, in which 1254 genes were upregulation while 731 genes were downregulation (Fig. 4D), were also depicted with a heat map (Fig. 4E). Applying GSEA indicated that immune-related pathways, such as the B cell receptor signaling pathway and natural killer cell-mediated cytotoxicity, were enriched in atherosclerosis plaque (Fig. 4F). We also performed the GO functional enrichment analysis for up and down differentially expressed genes in each of datasets (Fig. S3). Considering that if there were shared metabolism disturbances, the GSVA analyses were further performed and suggested that the metabolism of lipids and phospholipid metabolism pathways were up-regulated in NAFLD and AS diseases (Fig. 4G and H).

3.5. The identification of 7 shared risk genes for NAFLD and AS

Using WGCNA analysis discovered some modules were positively correlating with the severity or progression of disorders, in which some DEGs may trigger the diseases. Therefore, we further intersected the up-regulated genes with the common module genes to explore the final common genes. As the Venn plot shows, there were seven shared risk genes (ACP5, TP53I3, RPS6KA1, TYMS, TREM2, CA12, and IFI27) between NAFLD and atherosclerosis plaque (Fig. 5A and Table 3). Their PPI network, co-expression, or genetic interaction genes were constructed in the GeneMANIA database (Fig. 5B). To further elucidate the probable regulatory network, using the RegNetwork [32] to predict the TF-miRNA co-regulatory network and indicated that RPS6KA1 was targeted by the most TF/miRNAs, while no TF/miRNAs target IFI27 (Fig. 5C). In addition, we try to find the protein-chemical pairs (Table S3), which may help to discover the potential drugs or components for future interventions for developing multiple interventions or treating both diseases.

3.6. The shared risk genes displayed good diagnostic ability in NAFLD and AS plaque

To prove the reliability of these 7 shared risk genes at expression levels, we analyzed their expression in discovery cohorts and two external validation datasets. For NAFLD, all 7 genes were significantly up-regulated in GSE89632 and overexpressed along with the NAFLD activity score increased in GSE130970, while ACP5, TYMS, and TREM2 did not show significant expression although presenting up-regulated trends in GSE48452 (Fig. 6A–C). Interestingly, all these genes were significantly up-regulated in atherosclerosis plaque-related datasets GSE100927, GSE28829, and GSE43292 (Fig. 6D–F). Moreover, the ROC curves of the seven shared risk genes displayed good diagnostic ability in NAFLD (Fig. 7A and B and Table S4) and atherosclerosis plaque (Fig. 7C–E and Table S4), indicating the roust reliability of our results.

3.7. The different landscapes of immune cells between NAFLD and AS

According to our above results and existing studies that have shown immunity plays a crucial role in the initiation and development of both NAFLD and AS, we performed the CIBERSORT algorithm to discover the immune cells' abundance in different samples. The relative percentage of 22 immune subpopulations in each sample was visualized with bar plots in GSE89632 (Fig. 8A) and GSE100927 (Fig. 8C). Ranking immunocyte types of all samples in order of abundance indicated macrophages M2 was the most abundant immune cell type in both datasets (Fig. S4). Besides, comparing the abundance of different immune cells between diseases and controls indicated most immune cells were significantly dysregulated. Naïve B cells, plasma cells, and monocytes were down-regulated, whereas the γδ T cells were activated in both disorders (Fig. 8B and D).

Moreover, we calculated relationships between shared genes and immune cells and exhibited their correlations with heat maps (Fig. 9A and B). The cell-genes pairs with a grey or black background were significant, while those with white background were insignificant. TYMS was most positively and negatively correlated with M2 macrophages and naïve B cells in the NAFLD GSE89632,
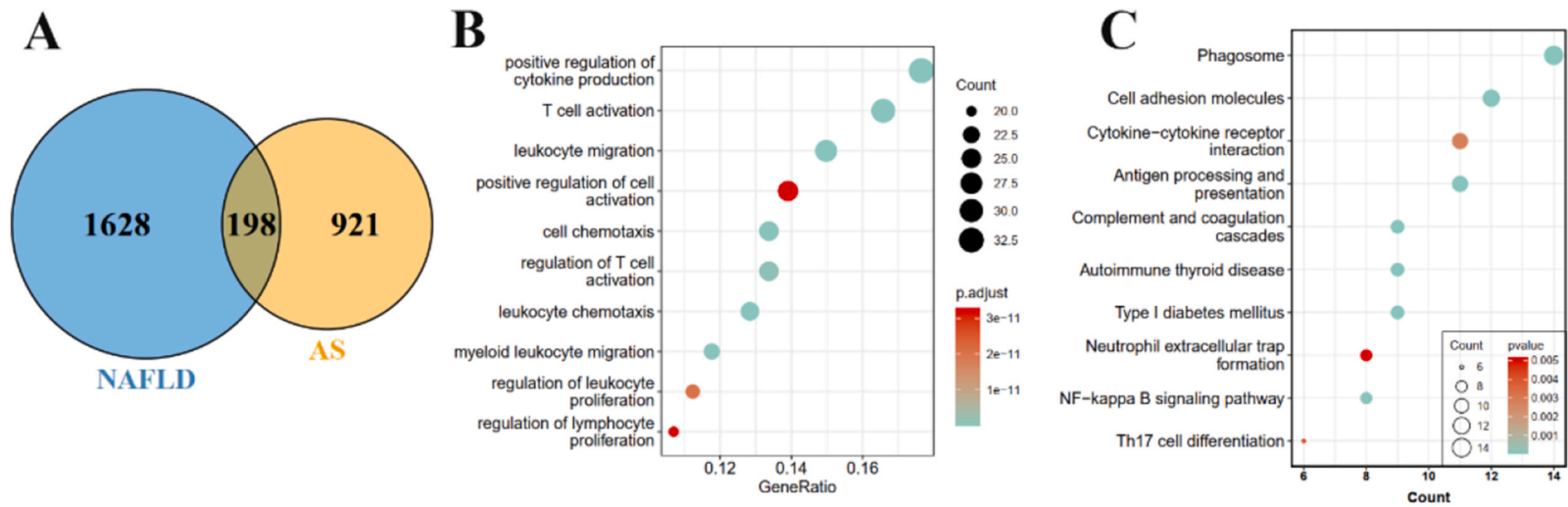
Fig. 3. Screening the common module genes and enrichment analysis. (A) A Venn plot showing 198 overlapped modules genes. (B) GO: BP and (C) KEGG enrichment analysis of 198 genes.
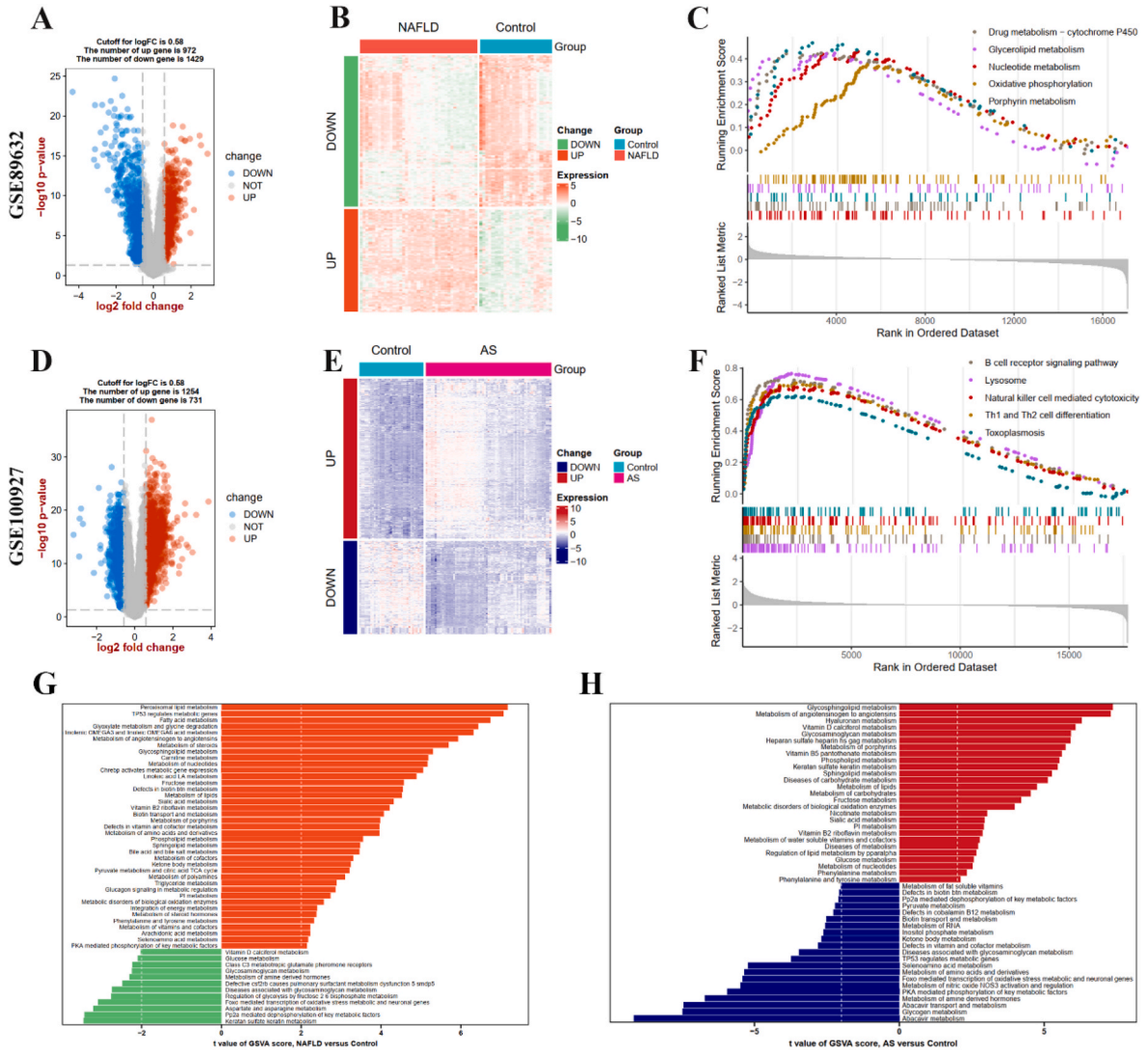
Fig. 4. DEGs analysis. (A) and (D) A volcano plot depicting the DEGs between diseases and controls in GSE89632 and GSE100927 datasets, respectively. (B) and (E) An heat map showing the expression patterns of DEGs in GSE89632 and GSE100927 datasets, respectively. (C) and (F) The GSEA analysis in GSE89632 and GSE100927 datasets, respectively. (G) and (H) The GSVA analysis to explore the metabolism-related pathways in GSE89632 and GSE100927 datasets, respectively.

respectively. Yet, for the AS GSE100927, ACP5 was most positively and negatively associated with M0 macrophages and CD4+ T cell memory resting, respectively.

The unique expression profiles of shared risk genes in metabolism/immune-related pathways showed by the sc-RNA-seq analysis of NAFLD and AS plaque.

We downloaded two single-cell RNA sequencing datasets: the GSE179886 dataset from PBMCs of one NAFLD and one healthy control and the GSE159677 dataset from three AC plaques and matched PA tissue of patients. After quality control and integration (Fig. S5), the Uniform Manifold Approximation and Projection (UMAP) was applied for nonlinear dimension reduction. A total of 11 and 13 clusters were identified by using the "FindCluster" function (Fig. 10A and D) in GSE179886 and GSE159677, respectively. Next, we performed cell annotation by using the "SingleR" package for the GSE179886 (Fig. 10B) and manually according to the expression of cell type marker genes for GSE159677 (Fig. S6 and Fig. 10E). Then, we visualized the expression and distribution of seven shared genes in different cells by using the "FeaturePlot" function. The results showed high levels of RPS6KA1 and ACP5 expressed in most cell types. TP53I3 and TREM2 were in monocytes, TYMS was in T cells, and IFI27 had a relatively high expression rate in monocytes and T cells, while CA12 was not detected in GSE179886 (Fig. 10C). In atherosclerosis plaque, ACP5 and TYMS were highly expressed in all cell types, TP53I3 was highly expressed in vascular smooth muscle cells (VSMCs), macrophages and endothelium, PRS6KA1 was in T cells, TREM2 was in macrophages, CA12 was in fibromyocyte, and IFI27 was in endothelium GSE159677 dataset (Fig. 10F).

Furthermore, we depicted the proportion of different cell types with a Sankey plot from the perspective of single-cell analysis.
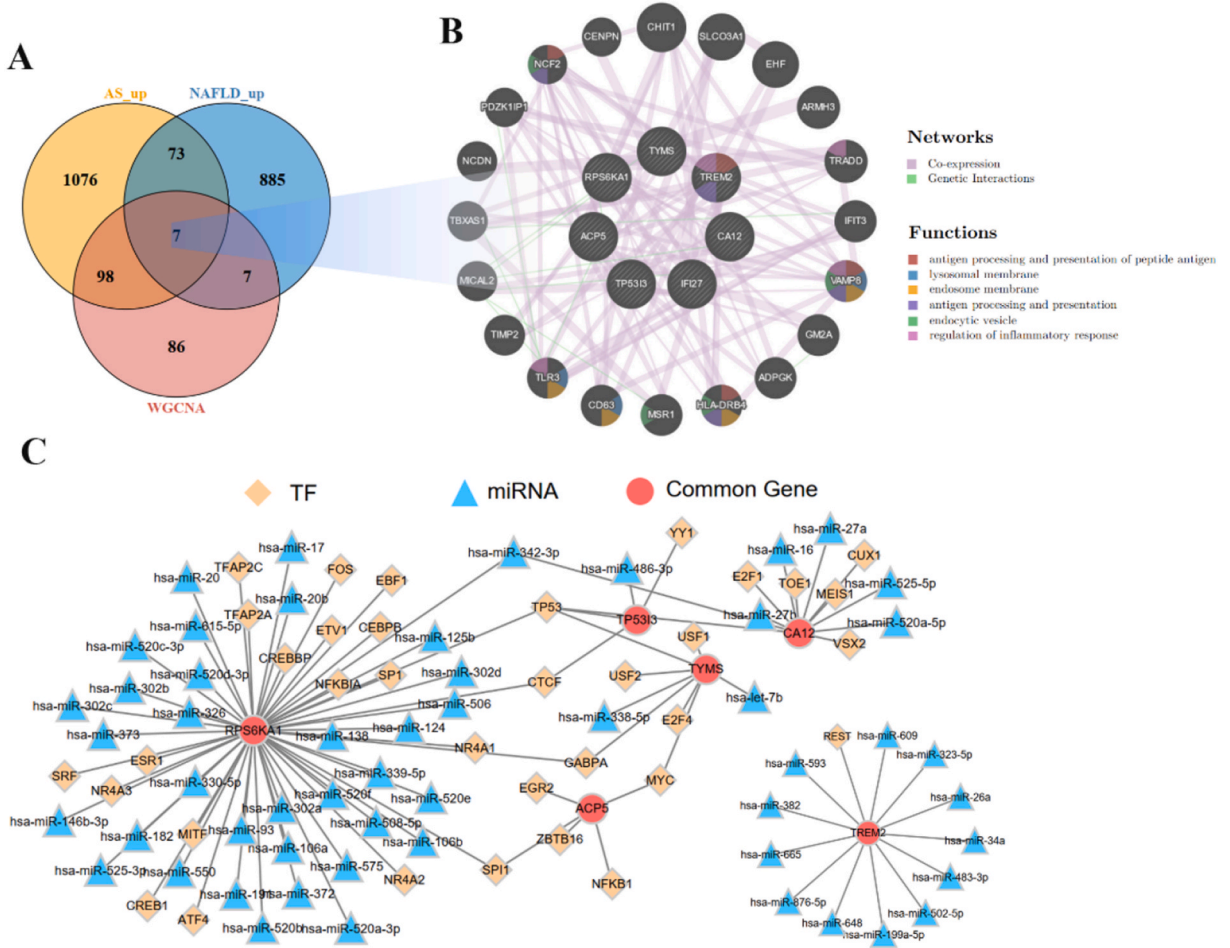
Fig. 5. Identification of shared risk genes between NAFLD and atherosclerosis plaques. (A) Seven shared risk genes by overlapping the up-regulated genes and module genes with a Venn diagram. (B) Protein-protein interactions of seven shared genes in GeneMANIA database. (C) Construction the TF-microRNAs co-regulatory network for seven shared genes. TF, transcription factors.

Monocytes and NK cells were decreasing and CD4 naïve T cells were increasing in NAFLD patients' PBMCs. At the AS core zones, the endothelium and fibromyocytes were decreasing with more macrophages and T lymphocytes (Fig. 11A). We also explore the difference in metabolism-related pathways between GSE179886 and GSE159677 by applying the "scMetabolism" package. Using the Wilcoxon test after the Benjamini-Hochberg adjustment, the significantly dysregulated metabolism-related pathways were identified and depicted with heat map (Fig. S7; Table S5 and Table S6). We extracted these pathways with similar up-reg ulated or down-regulated trends from controls to diseases (Fig. 11B). The results showed elevated fatty acid biosynthesis activity in both disorders, while that of fatty acid degradation and fatty acid elongation pathways was commonly decreased. Notably, there were significant correlations between these metabolism-related pathways with shared genes, implying these genes may play essential roles in regulating these processes (Fig. 11C and D).

4. Discussion

An epidemic of NAFLD has swept across the world. The growing burden of NAFLD presents enormous public health challenges and is a risk contributor to the global burden of atherosclerotic cardiovascular disease, which accounts for the majority of deaths worldwide. A large body of evidence has pinpointed the shared mechanisms that drive NAFLD and AS, while little research has called into question the common mechanisms of the two diseases from a gene-level perspective. Here, we enrolled 4851 non-Hispanic white participants aged 40–79 years from NHANES. Although the criteria for diagnosing NAFLD are not sufficiently precise, the FLI and the USFLI are noninvasive methods for assessing NAFLD that have been validated and utilized in previous research [38–40]. Based on this study population, we first demonstrated that NAFLD is significantly associated with an increased risk of ASCVD. Then, we conducted WGCNA to obtain co-expression modules of both disorders and found 198 potential risk genes. Meanwhile, we filtered out 2401 DEGs from the NAFLD dataset and 1985 DEGs from the AS dataset. By intersecting the up-regulated DEGs and 198 key-modules genes, we generated the final seven common risk DEGs (*ACP5*, *CA12*, *IFI27*, *RPS6KA1*, *TP53I3*, *TREM2*, and *TYMS*). Undoubtedly, these hub

Table 3
The detailed information about the seven shared genes.

Gene	Protein name	Protein function	Ch[a]	Gene Synonym
ACP5[b]	Tartrate-resistant acid phosphatase type 5	Involved in osteopontin/bone sialoprotein dephosphorylation. Its expression seems to increase in certain pathological states such as Gaucher and Hodgkin diseases, the hairy cell, the B-cell, and the T-cell leukemias. (https://www.uniprot.org/uniprotkb/P13686/entry)	19	HPAP
TP53I3[b]	tumor protein p53 inducible protein 3 (Quinone oxidoreductase PIG3)	Catalyzes the NADPH-dependent reduction of quinones. Exhibits a low enzymatic activity with beta-naphthoquinones, with a strong preference for the ortho-quinone isomer (1,2-beta-naphthoquinone) over the para isomer (1,4-beta-naphthoquinone). Also displays a low reductase activity for non-quinone compounds such as diamine and 2,6-dichloroindophenol (in vitro). Involved in the generation of reactive oxygen species (ROS). (https://www.uniprot.org/uniprotkb/Q53FA7/entry)	2	PIG3
RPS6KA1[b]	Ribosomal protein S6 kinase alpha-1	Serine/threonine-protein kinase that acts downstream of ERK (MAPK1/ERK2 and MAPK3/ERK1) signaling and mediates mitogenic and stress-induced activation of the transcription factors CREB1, ETV1/ER81 and NR4A1/NUR77, regulates translation through RPS6 and EIF4B phosphorylation, and mediates cellular proliferation, survival, and differentiation by modulating mTOR signaling and repressing pro-apoptotic function of BAD and DAPK1. (https://www.uniprot.org/uniprotkb/Q15418/entry)	1	HU-1
TYMS[b]	Thymidylate synthase	Catalyzes the reductive methylation of 2′-deoxyuridine 5′-monophosphate (dUMP) to thymidine 5′-monophosphate (dTMP), using the cosubstrate, 5,10-methylenetetrahydrofolate (CH2H4folate) as a 1-carbon donor and reductant and contributes to the de novo mitochondrial thymidylate biosynthesis pathway. (https://www.uniprot.org/uniprotkb/P04818/entry)	18	HsT422
TREM2[b]	Triggering receptor expressed on myeloid cells 2	Forms a receptor signaling complex with TYROBP which mediates signaling and cell activation following ligand binding. Acts as a receptor for amyloid-beta protein 42, a cleavage product of the amyloid-beta precursor protein APP, and mediates its uptake and degradation by microglia. (https://www.uniprot.org/uniprotkb/Q9NZC2/entry)	6	TREM-2
CA12[b]	Carbonic anhydrase 12	Reversible hydration of carbon dioxide. (https://www.uniprot.org/uniprotkb/O43570/entry)	15	HsT18816
IFI27[b]	Interferon alpha-inducible protein 27	Probable adapter protein involved in different biological processes. (https://www.uniprot.org/uniprotkb/P40305/entry)	14	FAM14D

[a] Ch: Chromosome.
[b] The gene type is protein_coding.

genes showed good diagnostic ability for both diseases. Furthermore, we mapped up the landscapes of the immune and metabolism of NAFLD and AS. Of note, the aforementioned seven genes showed pathological changes in the immune cells by dissecting single-cell sequencing datasets and significantly correlated with shared metabolic pathways in both diseases [20].

Available evidence suggests that three hub genes, *ACP5*, *CA12* and *IFI27,* are primarily associated with AS. ACP5, also known as tartrate-resistant acid phosphatase (TRAP), is a metalloprotein enzyme that belongs to the acid phosphatase family. Although the role in NAFLD is unclear, ACP5 has been proven to promote atherogenesis, in which a higher serum ACP5 level was accompanied by more serious AS [41,42]. Considering NAFLD and AS shared multiple metabolic pathways, we speculate that ACP5 may drive NAFLD and AS by resulting in a worse atherogenic lipoprotein profile [41,42]. Similar to ACP5, *CA12* (carbonic anhydrase 12) was highly expressed in advanced AS, which was identified by another bioinformatics study [43] and is in line with our findings. However, the pathological mechanism of CA12 in NAFLD and AS remained unknown. CA12 could be expressed by osteoclasts, and regulate the accumulation and functions of macrophages in tumor microenvironments [44]. Macrophages play a key role in atherogenesis, such as transforming into foam cells, secreting inflammatory cytokines and regulating immunity. Therefore, it's reasonable to deduce CA12 may also involve in the progression of NAFLD and AS through regulating macrophage functions. So far, the links between IFI27 and NAFLD have not been reported yet. As an interferon-a highly inducible protein, IFI27 was upregulated in endothelial progenitor cells (EPCs) in response to monomeric CRP, which contributes to AS by triggering local inflammation and negatively affecting EPC numbers and functions [45]. IFI27 was often involved in the interferon-gamma signaling pathway and innate immune response [46]. Consistent with this, IFI27 might drive the common immunomodulation in both diseases.

In addition, previous studies have demonstrated the other 4 risk genes (*RPS6KA1*, *TP53I3*, *TREM2*, and *TYMS*) contribute to the occurrence of NAFLD or AS, especially for NAFLD. RPS6K1 (the ribosomal protein S6 kinase 1) is a downstream effector of mTORC1, known for regulating lipid homeostasis [47], which is important for both NAFLD and AS. Diminishing RPS6K1 activity not only hampered the expansion of fat mass but also alleviated hepatic steatosis and dyslipidemia [48]. TREM2 is a cell-surface lipid-binding receptor, which transduces intracellular signals through the adaptor DAP12. Its deficiency may lead to dysregulated gene expression of lipid metabolism and impairment of lipid handling function [49]. Indeed, a significantly increased steatosis was found in advanced MCD-induced NASH and HFC-induced NAFLD models [50], which was in accordance with our findings. The abnormalities in energy and biosynthesis have emerged as the central player in NAFLD. TP5313, a well-established p53-regulated gene, could activate NADPH quinone oxidoreductase, which has been assumed to be tightly connected to NAFLD [51], whereas the role of TP5313 in AS has not
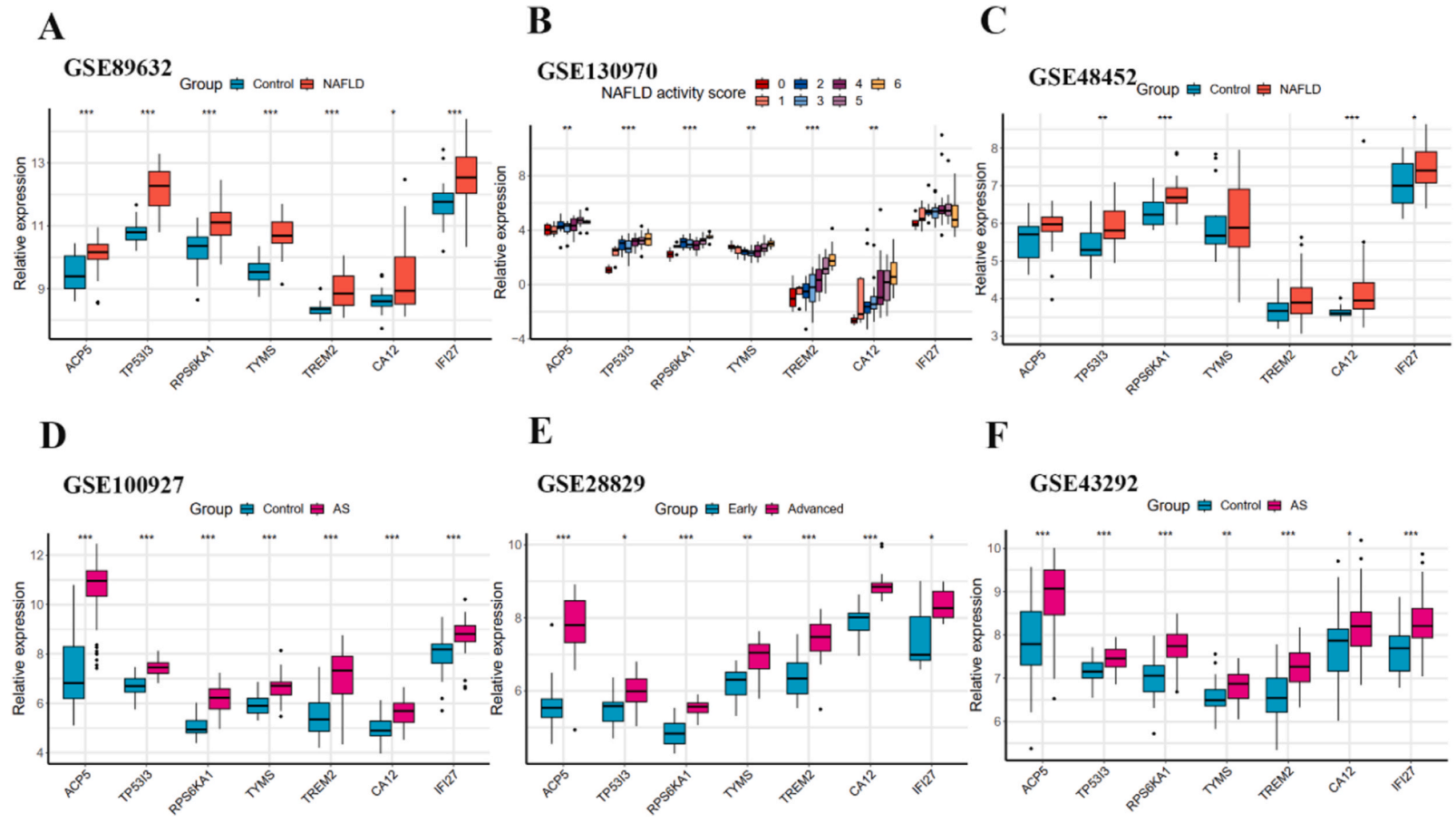
Fig. 6. The expression levels of the seven hub genes in NAFLD datasets (GSE89632, GSE130970, and GSE48452; A-C) and atherosclerosis plaque datasets (GSE100927, GSE28829, and GSE43292; D-F).
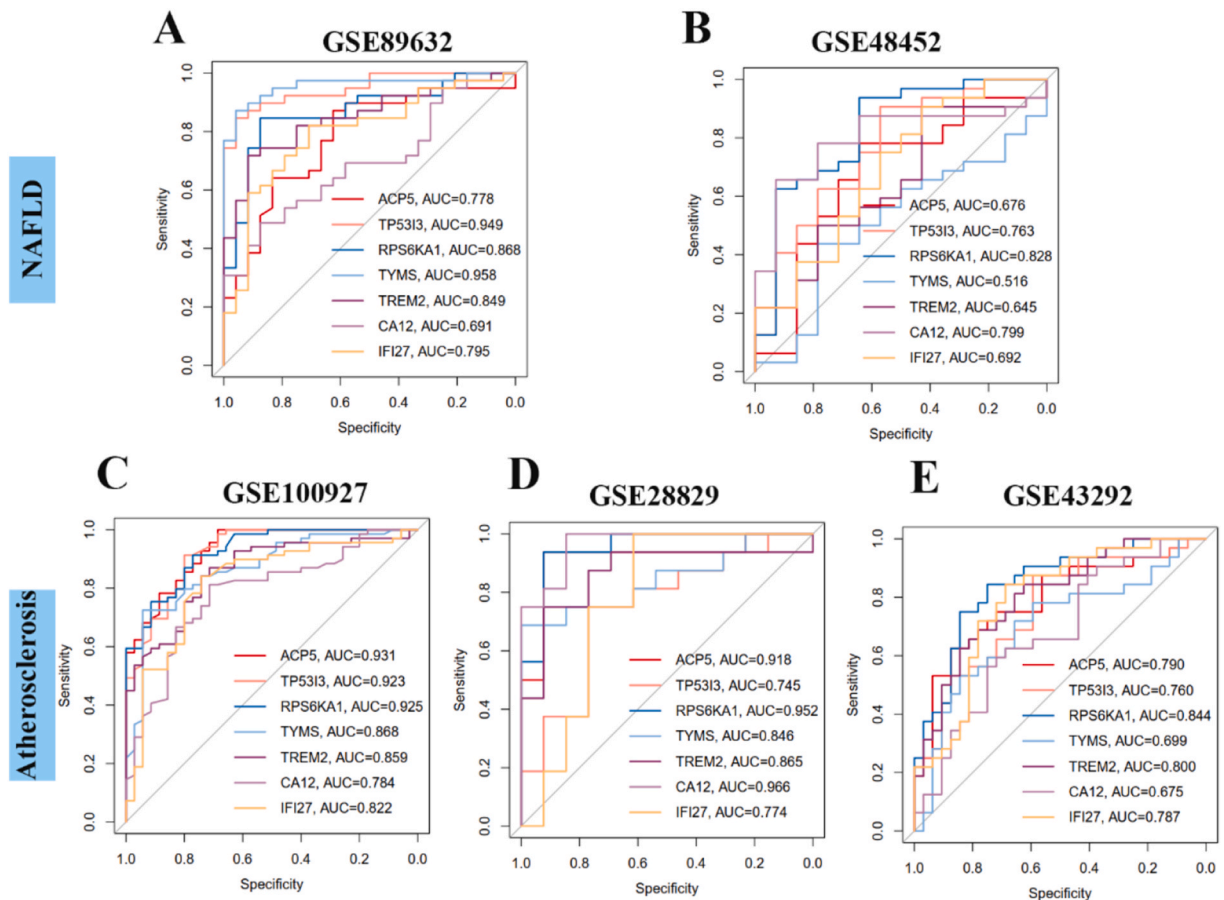
Fig. 7. The diagnosis of seven shared genes in the NAFLD datasets (GSE89632 and GSE48452; A-B) and atherosclerosis plaque datasets (GSE100927, GSE28829, and GSE43292; C-E).

been clarified. Thymidylate (TYMS) is an essential substrate of DNA synthesis synthase, which plays a key role in biosynthesizing thymidine monophosphate. A recent study highlights high levels of TYMS in NASH and NAFLD patients [52], which is similar to ours. In a nutshell, the risk gene's biological functions are congruent with the characteristics of NAFLD and AS, emphasizing their potential roles and significance in the pathogenesis of NAFLD and AS.

In the formation of NAFLD and AS, a massive of immunological responses are triggered, including immune cell activation and cytokine production, forming a nearly integrated immune circuit ultimately. Inspired by the biological significance of immunity in NAFLD and AS, we carried out an immune cell infiltration analysis. The CIBERSORT result revealed different immune cell abundance in NAFLD and AS samples, with the macrophages being the most abundant. The single-cell data further linked the seven shared risk gene patterns to diverse immune cell subsets, and the TYMS and ACP5 showed the most positive correlation with M2 macrophages and M0 macrophages, respectively. These reference expression patterns concerning disease status may be of utility in ascertaining key immune cell subsets for both NAFLD and AS.

Nowadays, it's well-established that both innate and adaptive immunity are involved in NAFLD and AS [53]. Macrophage is one of the most widely studied in the innate immune system. Macrophages proliferate rapidly in the liver during the early stages of NAFLD, boosting inflammatory responses and metabolic dysregulation [54]. This phenomenon was underscored by the observation of increased monocyte influx and monocyte-derived cell accumulation within the myeloid compartment in both mice and humans with NAFLD [55–57]. In AS, lipids are accumulated with subendothelial depositions, along with the high infiltration of cholesterol-loaded macrophages and T cells [53,58]. Consistent with our results, patients with hyperlipidemia and AS have shown elevated levels of circulating monocytes, which serve as progenitors for macrophages and are strongly correlated with plaque size and progression [59, 60]. Our data further revealed that M2 macrophages were the predominant infiltrating cells in both illnesses. In fact, previous studies have demonstrated that the significant involvement of M2 macrophages in AS in both murine models and human plaques [61,62]. The role of M2 macrophages in early stable and active atherosclerotic plaques, highlighted their propensity to drive plaque regression [63, 64]. Moreover, recent studies also indicated an enhanced expression of liver anti-inflammatory M2 macrophages in the context of NASH and liver fibrosis in both NAFLD patients and murine models [65,66].

Our studies also emphasized the significance of T cells in NAFLD and AS. The balance of various T cells is critical for maintaining
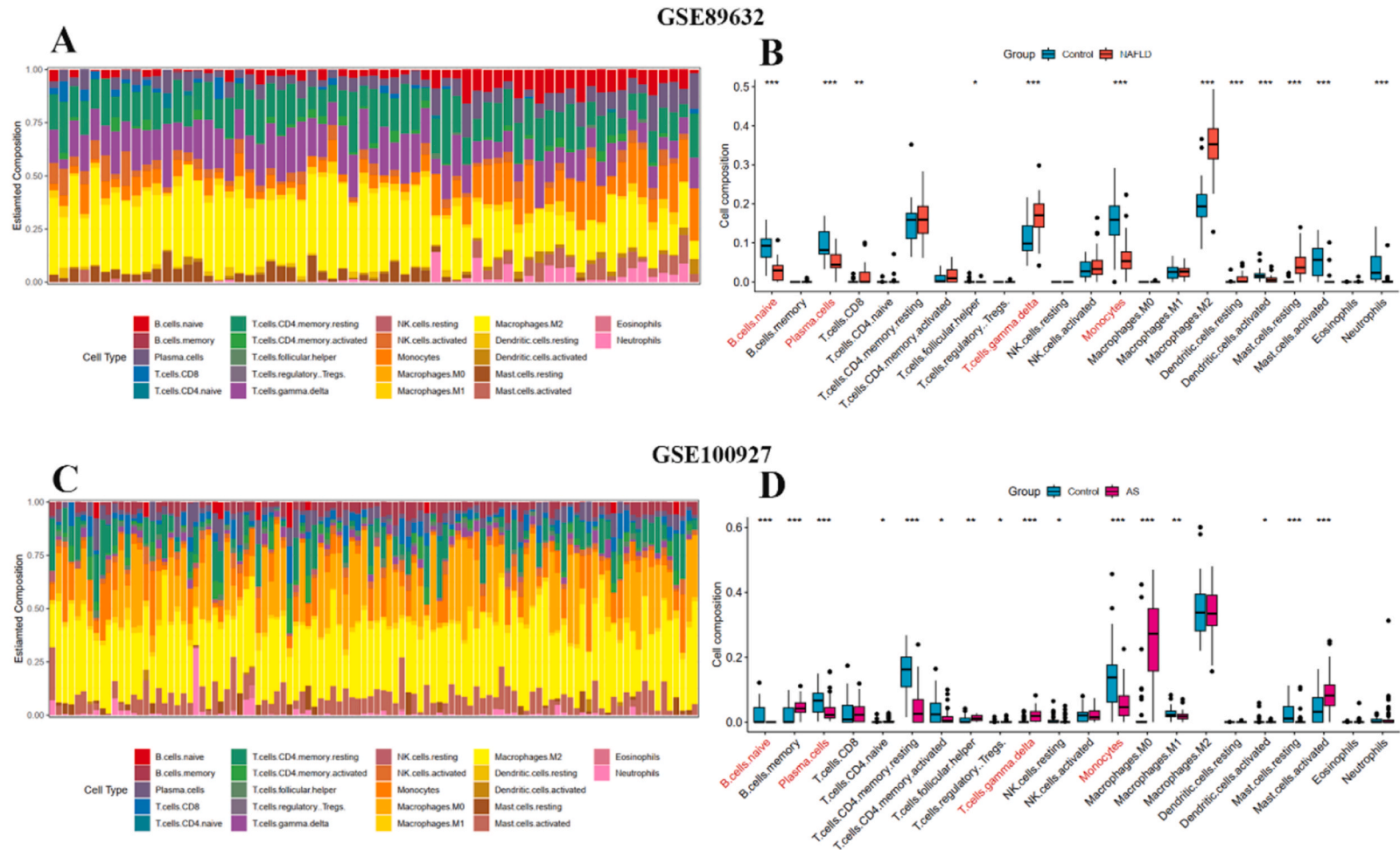
Fig. 8. The immune infiltration analysis. (A) The proportion of 22 type immune cells in each sample in GSE89632. (B) Boxplot comparing the abundance of the 22 type immune cells between NAFLD and controls. (C) The proportion of 22 type immune cells in each sample in GSE100932. (B) Boxplot comparing the abundance of the 22 type immune cells between AS and controls. NAFLD, non-alcoholic fatty liver disease; AS, atherosclerosis. *p-value <00.05, **p-value <00.01, ***p-value <00.001.
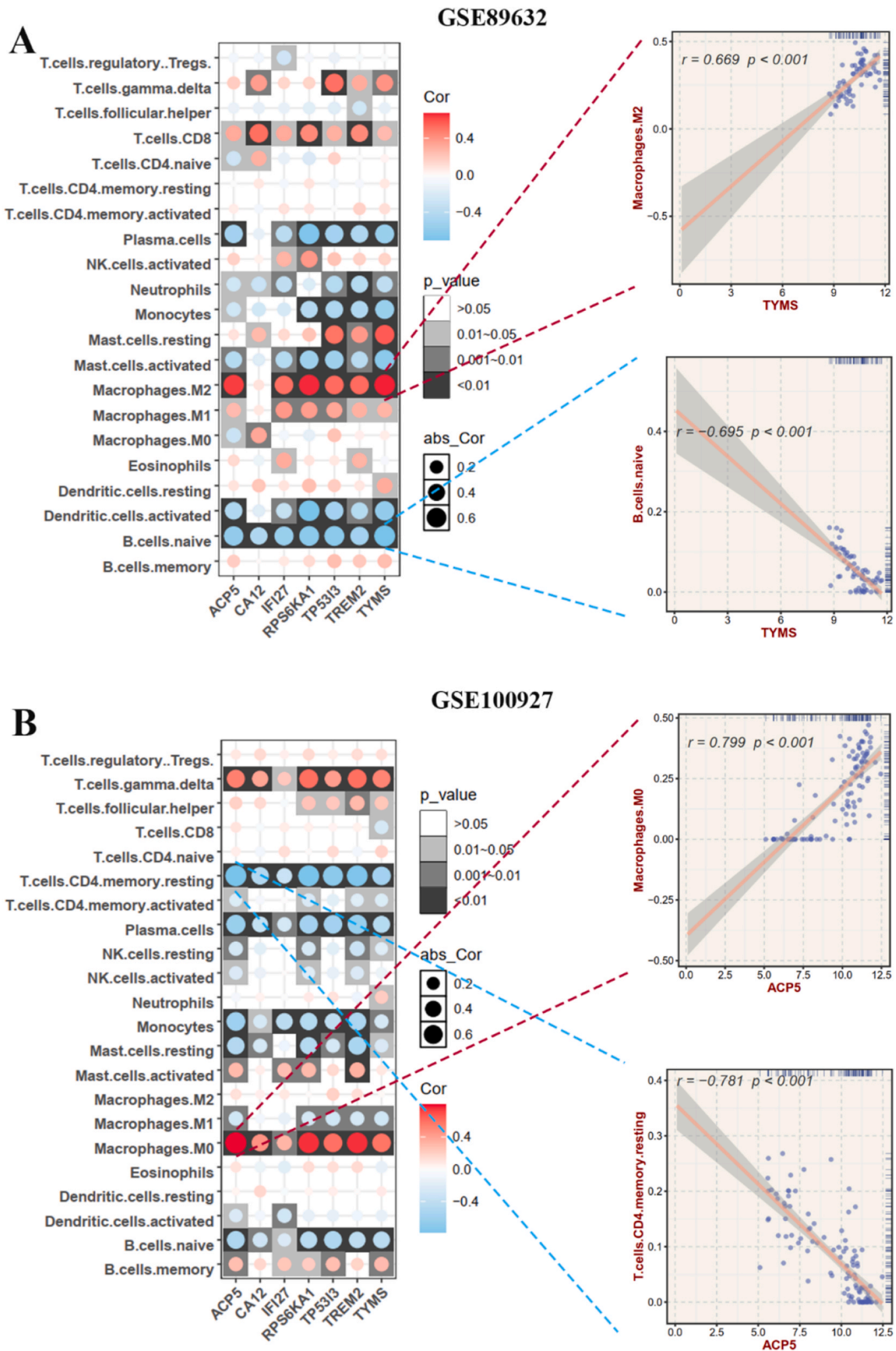
Fig. 9. The correlations between immune cells and the seven shared genes. (A) and (B) A heat map showing the associations between immune cells and the seven shared genes in GSE89632 and GSE100932 dataset. The size of the dot shows the absolute correlation coefficient. The white background represents the insignificant relationship. The two right panels indicate the most positive and negative correlation.
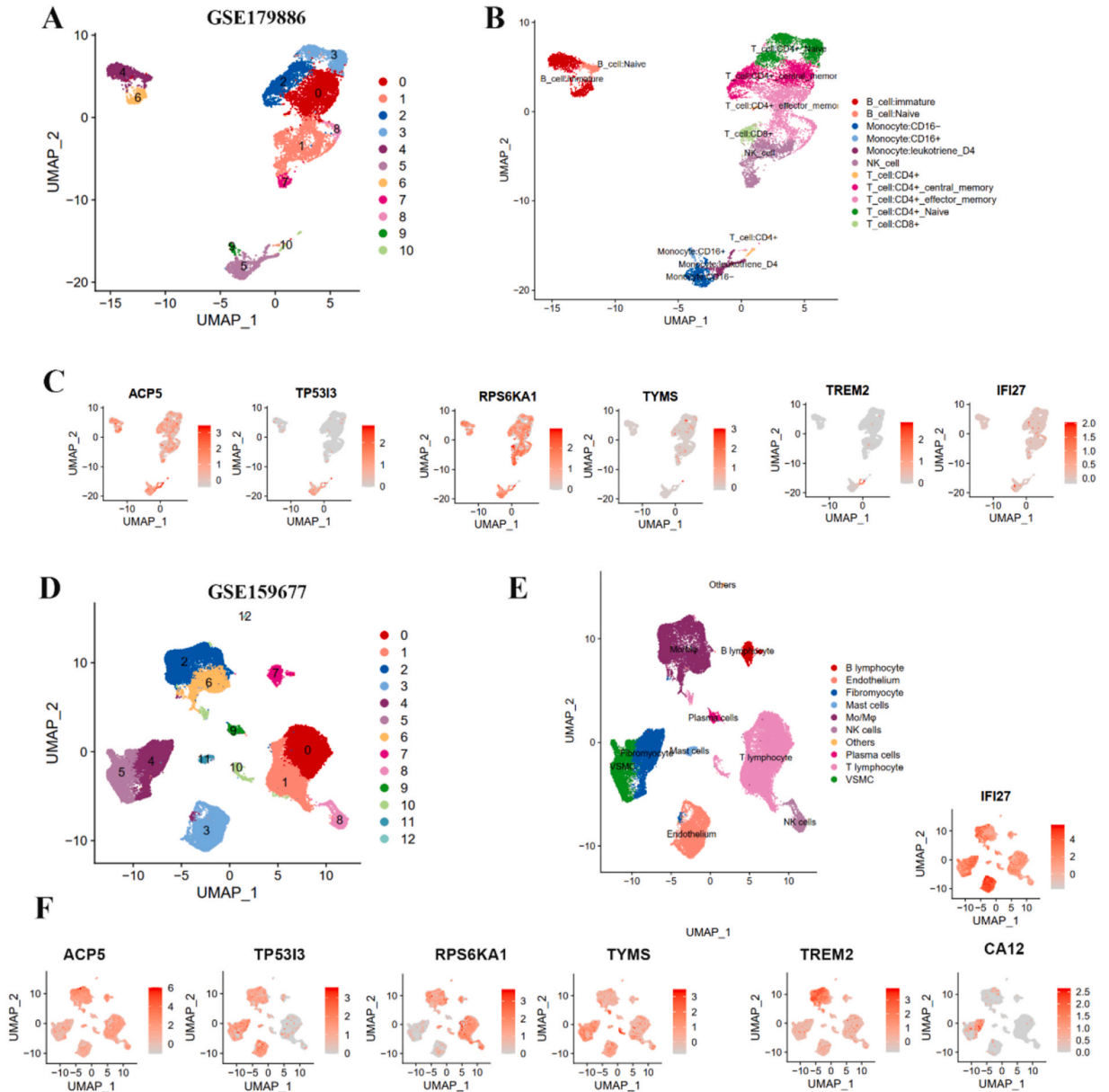
Fig. 10. The expression of seven shared genes in single-cell levels. (A) The cell clusters and (B) annotated cell types in GSE179886. (C) Feature plot indicating the expression and distribution of the shared genes in GSE179886. (D) The cell clusters and (E) annotated cell types in GSE159677. (F) Feature plot indicating the expression and distribution of the shared genes in GSE159677.
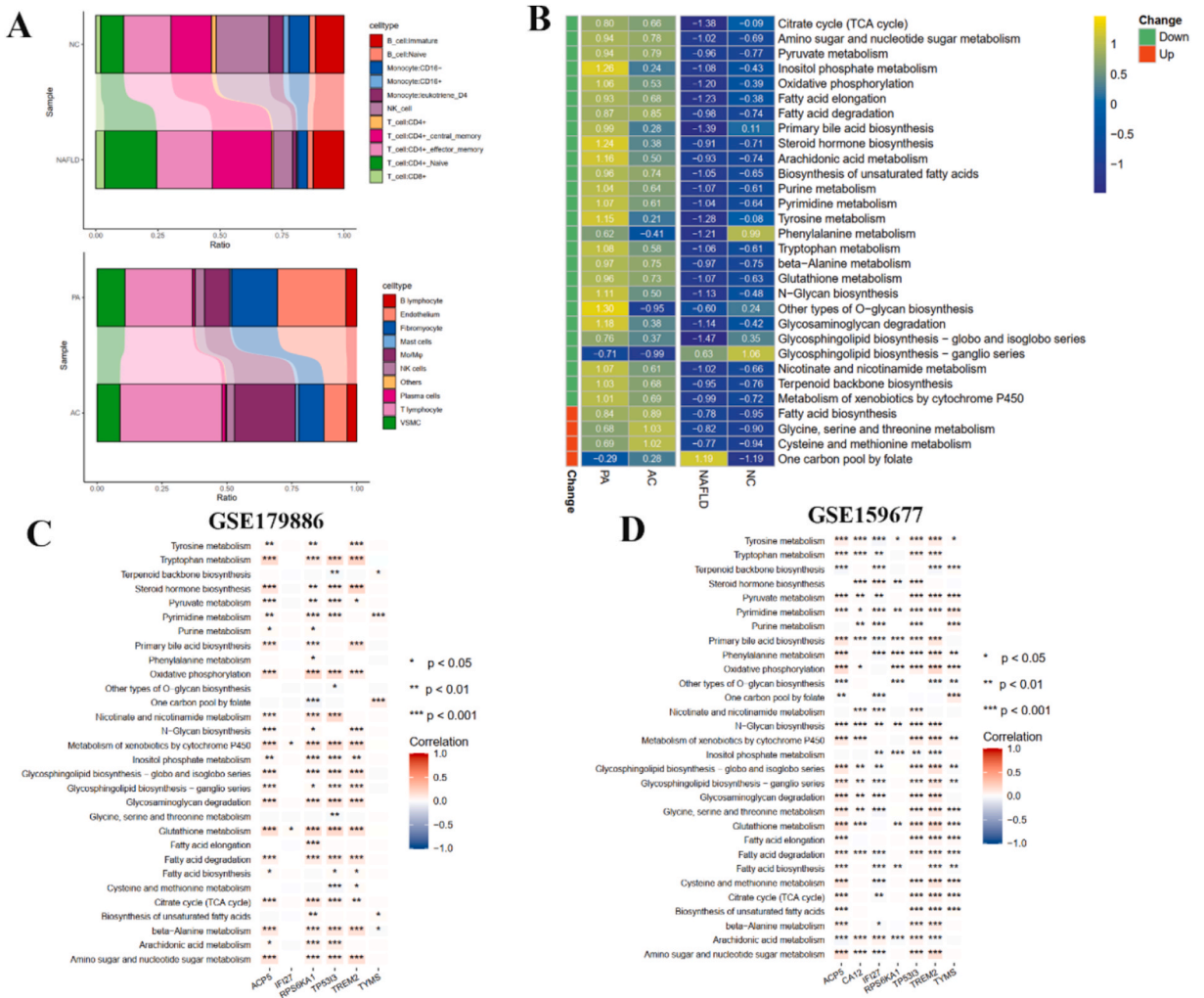
Fig. 11. The percentage of different cell types and metabolism-related pathways in GSE179886 and GSE159677. (A) The bar plot depicting the percentage of different cell types in GSE179886 (top) and GSE159677 (bottom). (B) The common metabolism-related pathways presenting with the same trends from controls to diseases. (C) and (D)The relationships between shared genes and common metabolism-related pathways in GSE179886 and GSE159677, respectively.

hepatic immune homeostasis [67]. There was a significant accumulation of CD4$^+$ T cells in the liver of a humanized mouse model with a high-fat diet [68]. In addition, marked hepatic infiltration of CD8$^+$ T lymphocytes was observed in patients with NASH disease [69]. Although CD8$^+$ T cells were low frequencies detected in the plaque, it could affect AS by promoting plaque inflammation and the formation of the necrotic core [19].

In addition to the immune response, our results highlighted the significance of fatty acid metabolism abnormality, which presented an enhanced fatty acid biosynthesis and downregulated fatty acid degradation and elongation pathways. Moreover, our study also revealed the potential role of glycerolipid metabolism and oxidative phosphorylation in two diseases. A retrospective study of NAFLD patients found that the most commonly changed metabolite families were glycerophospholipids, which are involved in PC, PA, PE, and PG [70]. The lipid metabolism disturbance results in fat accumulation in hepatocytes and further activates redox-sensitive transcription factors and proinflammatory mediators, which trigger the start of various immune-mediated mechanisms and further damage liver cells [71]. Recently, the human serum metabolomic study showed that phospholipase metabolism disturbances were closely related to the progression of NAFLD [72]. We believe that drugs targeting the metabolism pathway would have a protective effect on both illnesses [73,74].

In summary, our work validated the seven shared gene expression levels in discovery cohorts and two external validation datasets, which combined with existing reports further proved the robust reliability of our findings. Moreover, the ROC curves exhibited the excellent diagnostic power of the seven risk genes in both NAFLD and atherosclerosis plaque. The regulatory network showed that RPS6KA1 was the target of most TFs and miRNAs. Combined with protein-chemical networks may help to shed light on potential drugs

or components for future interventions that target both diseases simultaneously. However, there are also limitations of the study. First, the results of our study are based only on microarray data analysis, in which the genetic data is relatively limited. Second, the analysis results are still speculative. Although some innovations have been made in the methods and results, further basic and clinical research is needed to verify those key risk genes and signaling pathways, especially those that have not yet been reported. At lastly but not least, it is important to note that the exact current criteria for diagnosing NAFLD remain unclear. We believe that emerging concepts, such as the transition from NAFLD to MASLD, as well as new research findings, will ultimately benefit individuals affected by ASCVD and NAFLD.

5. Conclusion

In this study, through comprehensive utilizing the bulk and single-cell transcriptome analyses, we mined 7 shared risk genes (*ACP5*, *TP53I3*, *RPS6KA1*, *TYMS*, *TREM2*, *CA12*, and *IFI27*) with good diagnostic ability and depicted the unique landscapes of immune and metabolism for NAFLD and AS. We found that RPS6KA1 could be targeted by most TF/miRNAs, and might be a useful intervention target for treating both diseases simultaneously. Our results provided comprehensive insights into both disorders, paving the way for further basic research aiming to clarify the underlying links between them.

Ethics approval and consent for participants

Ethics approval and consent to participate in GEO and NHANES belong to public databases. The patients involved in the database have obtained ethical approval and consent. Users can download relevant data for free for research and publish relevant articles.

Data availability statement

The original contributions presented in the study are included in the article/Supplementary Material. Further inquiries can be directed to the corresponding authors. The NHANES data in this study is sourced from the Centers for Disease Control and Prevention, and all data is freely accessible at: https://wwwn.cdc.gov/Nchs/Nhanes/. The Gene Expression Omnibus (GEO) datasets were downloaded from the GEO website (https://www.ncbi.nlm.nih.gov/gds) and the code requests should be submitted to the corresponding author for consideration.

CRediT authorship contribution statement

Qian Hu: Writing – review & editing, Writing – original draft. **Yunfang Luo:** Writing – original draft, Methodology, Conceptualization. **Hao He:** Methodology. **Hua Chen:** Validation, Software. **Di Liao:** Writing – review & editing, Supervision.

Declaration of competing interest

The authors declare that they have no known competing financial interests or personal relationships that could have appeared to influence the work reported in this paper.

Appendix A. Supplementary data

Supplementary data to this article can be found online at https://doi.org/10.1016/j.heliyon.2024.e35453.

References

[1] A.S.o.N.C. From the American Association of Neurological Surgeons, C.I.R.A.C.o.N.S.E.S.o.M.I.N.T.E.S.o.N.E.S.O.S.f.C.A. Interventional Radiology Society of Europe, N.S. Interventions, O. World Stroke, D. Sacks, B. Baxter, B.C.V. Campbell, J.S. Carpenter, C. Cognard, D. Dippel, M. Eesa, U. Fischer, K. Hausegger, J. A. Hirsch, M. Shazam Hussain, O. Jansen, M.V. Jayaraman, A.A. Khalessi, B.W. Kluck, S. Lavine, P.M. Meyers, S. Ramee, D.A. Rufenacht, C.M. Schirmer, D. Vorwerk, Multisociety consensus quality improvement revised consensus statement for endovascular therapy of acute ischemic stroke, Int. J. Stroke 13 (2018) 612–632, https://doi.org/10.1177/1747493018778713.

[2] N. Chalasani, Z. Younossi, J.E. Lavine, M. Charlton, K. Cusi, M. Rinella, S.A. Harrison, E.M. Brunt, A.J. Sanyal, The diagnosis and management of nonalcoholic fatty liver disease: practice guidance from the American Association for the Study of Liver Diseases, Hepatology (Baltimore, Md 67 (2018) 328–357, https://doi.org/10.1002/hep.29367.

[3] D.Q. Huang, H.B. El-Serag, R. Loomba, Global epidemiology of NAFLD-related HCC: trends, predictions, risk factors and prevention, Nat. Rev. Gastroenterol. Hepatol. 18 (2021) 223–238, https://doi.org/10.1038/s41575-020-003816.

[4] M.E. Rinella, Nonalcoholic fatty liver disease: a systematic review, JAMA 313 (2015) 2263–2273, https://doi.org/10.1001/jama.2015.5370.

[5] M.I. Elsaid, Y. Li, J.F.P. Bridges, G. Brock, C.D. Minacapelli, V.K. Rustgi, Association of bariatric surgery with cardiovascular outcomes in adults with severe obesity and nonalcoholic fatty liver disease, JAMA Netw. Open 5 (2022) e2235003, https://doi.org/10.1001/jamanetworkopen.2022.35003.

[6] A. Ismaiel, O.S. Ciobanu, M. Ismaiel, D.C. Leucuta, S.L. Popa, L. David, D. Ensar, N. Al Srouji, D.L. Dumitrascu, Atherogenic index of plasma in non-alcoholic fatty liver disease: systematic review and meta-analysis, Biomedicines 10 (2022), https://doi.org/10.3390/biomedicines10092101.

[7] T. Arai, M. Atsukawa, A. Tsubota, K. Kato, H. Abe, H. Ono, T. Kawano, Y. Yoshida, T. Tanabe, T. Okubo, K. Hayama, A. Nakagawa-Iwashita, N. Itokawa, C. Kondo, K. Kaneko, N. Emoto, M. Nagao, K. Inagaki, I. Fukuda, H. Sugihara, K. Iwakiri, Liver fibrosis is associated with carotid atherosclerosis in patients with liver biopsy-proven nonalcoholic fatty liver disease, Sci. Rep. 11 (2021) 15938, https://doi.org/10.1038/s41598-021-95581-8.

[8] H. Tilg, M. Effenberger, From NAFLD to MAFLD: when pathophysiology succeeds, Nature reviews, Gastroenterol. Hepatol. 17 (2020) 387–388, https://doi.org/10.1038/s41575-020-03166.

[9] M. Eslam, A.J. Sanyal, J. George, P. International Consensus, MAFLD: a consensus-driven proposed nomenclature for metabolic associated fatty liver disease, Gastroenterology 158 (2020) 1999–2014 e1991, https://doi.org/10.1053/j.gastro.2019.11.312.

[10] M. Eslam, P.N. Newsome, S.K. Sarin, Q.M. Anstee, G. Targher, M. Romero-Gomez, S. Zelber-Sagi, V. Wai-Sun Wong, J.F. Dufour, J.M. Schattenberg, T. Kawaguchi, M. Arrese, L. Valenti, G. Shiha, C. Tiribelli, H. Yki-Jarvinen, J.G. Fan, H. Gronbaek, Y. Yilmaz, H. Cortez-Pinto, C.P. Oliveira, P. Bedossa, L. A. Adams, M.H. Zheng, Y. Fouad, W.K. Chan, N. Mendez-Sanchez, S.H. Ahn, L. Castera, E. Bugianesi, V. Ratziu, J. George, A new definition for metabolic dysfunction-associated fatty liver disease: an international expert consensus statement, J. Hepatol. 73 (2020) 202–209, https://doi.org/10.1016/j.jhep.2020.03.039.

[11] Q. Xiang, F. Tian, J. Xu, X. Du, S. Zhang, L. Liu, New insight into dyslipidemia-induced cellular senescence in atherosclerosis, Biol Rev Camb Philos Soc 97 (2022) 1844–1867, https://doi.org/10.1111/brv.12866.

[12] P. Libby, J.E. Buring, L. Badimon, G.K. Hansson, J. Deanfield, M.S. Bittencourt, L. Tokgozoglu, E.F. Lewis, Atherosclerosis, Nat Rev Dis Primers 5 (2019) 56, https://doi.org/10.1038/s41572-019-0106-z.

[13] P.B. Duell, F.K. Welty, M. Miller, A. Chait, G. Hammond, Z. Ahmad, D.E. Cohen, J.D. Horton, G.S. Pressman, P.P. Toth, T. American Heart Association Council on Arteriosclerosis, B. Vascular, H. Council on, D. Council on the Kidney in Cardiovascular, L. Council on, H. Cardiometabolic, D. Council on Peripheral Vascular, Nonalcoholic fatty liver disease and cardiovascular risk: a scientific statement from the American heart association, Arterioscler. Thromb. Vasc. Biol. 42 (2022) e168–e185, https://doi.org/10.1161/ATV.0000000000000153.

[14] A.S.P. Tang, K.E. Chan, J. Quek, J. Xiao, P. Tay, M. Teng, K.S. Lee, S.Y. Lin, M.Z. Myint, B. Tan, V.K. Sharma, D.J.H. Tan, W.H. Lim, A. Kaewdech, D. Huang, N. W. Chew, M.S. Siddiqui, A.J. Sanyal, M. Muthiah, C.H. Ng, Non-alcoholic fatty liver disease increases risk of carotid atherosclerosis and ischemic stroke: an updated meta-analysis with 135,602 individuals, Clin. Mol. Hepatol. 28 (2022) 483–496, https://doi.org/10.3350/cmh.2021.0406.

[15] D. Stols-Goncalves, G.K. Hovingh, M. Nieuwdorp, A.G. Holleboom, NAFLD and atherosclerosis: two sides of the same dysmetabolic coin? Trends in endocrinology and metabolism: TEM (Trends Endocrinol. Metab.) 30 (2019) 891–902, https://doi.org/10.1016/j.tem.2019.08.008.

[16] T. Huby, E.L. Gautier, Immune cell-mediated features of non-alcoholic steatohepatitis, Nat. Rev. Immunol. 22 (2022) 429–443, https://doi.org/10.1038/s41577-021-00639-3.

[17] F. Abdolmaleki, S.M. Gheibi Hayat, V. Bianconi, T.P. Johnston, A. Sahebkar, Atherosclerosis and immunity: a perspective, Trends Cardiovasc. Med. 29 (2019) 363–371, https://doi.org/10.1016/j.tcm.2018.09.017.

[18] P. Roy, M. Orecchioni, K. Ley, How the immune system shapes atherosclerosis: roles of innate and adaptive immunity, Nat. Rev. Immunol. 22 (2022) 251–265, https://doi.org/10.1038/s41577-021-00584-1.

[19] D. Wolf, K. Ley, Immunity and inflammation in atherosclerosis, Circ. Res. 124 (2019) 315–327, https://doi.org/10.1161/CIRCRESAHA.118.313591.

[20] P. Libby, The changing landscape of atherosclerosis, Nature 592 (2021) 524–533, https://doi.org/10.1038/s41586-021-033928.

[21] D.C. Goff Jr., D.M. Lloyd-Jones, G. Bennett, S. Coady, R.B. D'Agostino, R. Gibbons, P. Greenland, D.T. Lackland, D. Levy, C.J. O'Donnell, J.G. Robinson, J. S. Schwartz, S.T. Shero, S.C. Smith Jr., P. Sorlie, N.J. Stone, P.W. Wilson, H.S. Jordan, L. Nevo, J. Wnek, J.L. Anderson, J.L. Halperin, N.M. Albert, B. Bozkurt, R. G. Brindis, L.H. Curtis, D. DeMets, J.S. Hochman, R.J. Kovacs, E.M. Ohman, S.J. Pressler, F.W. Sellke, W.K. Shen, S.C. Smith Jr., G.F. Tomaselli, G. American College of Cardiology/American Heart Association Task Force on Practice, ACC/AHA guideline on the assessment of cardiovascular risk: a report of the American college of cardiology/American heart association task force on practice guidelines, Circulation 129 (2014) S49–S73, https://doi.org/10.1161/01.cir.0000437741.48606.98, 2013.

[22] G. Bedogni, S. Bellentani, L. Miglioli, F. Masutti, M. Passalacqua, A. Castiglione, C. Tiribelli, The Fatty Liver Index: a simple and accurate predictor of hepatic steatosis in the general population, BMC Gastroenterol. 6 (2006) 33, https://doi.org/10.1186/1471-230X-6-33.

[23] C.E. Ruhl, J.E. Everhart, Fatty liver indices in the multiethnic United States national health and nutrition examination Survey, Aliment. Pharmacol. Ther. 41 (2015) 65–76, https://doi.org/10.1111/apt.13012.

[24] T. Barrett, S.E. Wilhite, P. Ledoux, C. Evangelista, I.F. Kim, M. Tomashevsky, K.A. Marshall, K.H. Phillippy, P.M. Sherman, M. Holko, A. Yefanov, H. Lee, N. Zhang, C.L. Robertson, N. Serova, S. Davis, A. Soboleva, NCBI GEO: archive for functional genomics data sets–update, Nucleic Acids Res. 41 (2013) D991–D995, https://doi.org/10.1093/nar/gks1193.

[25] S. Li, Q. Zhang, Z. Huang, W. Tao, C. Zeng, L. Yan, F. Chen, Comprehensive analysis of immunocyte infiltration and the key genes associated with intraplaque hemorrhage in carotid atherosclerotic plaques, Int Immunopharmacol 106 (2022) 108633, https://doi.org/10.1016/j.intimp.2022.108633.

[26] S. Li, Q. Zhang, L. Weng, J. Li, Construction of an immune-related signature for predicting the ischemic events in patients undergoing carotid endarterectomy, Front. Genet. 13 (2022) 1014264, https://doi.org/10.3389/fgene.2022.1014264.

[27] P. Langfelder, S. Horvath, WGCNA: an R package for weighted correlation network analysis, BMC Bioinf. 9 (2008) 559, https://doi.org/10.1186/1471-2105-9-559.

[28] M.E. Ritchie, B. Phipson, D. Wu, Y. Hu, C.W. Law, W. Shi, G.K. Smyth, Limma powers differential expression analyses for RNA-sequencing and microarray studies, Nucleic Acids Res. 43 (2015) e47, https://doi.org/10.1093/nar/gkv007.

[29] G. Yu, L.G. Wang, Y. Han, Q.Y. He, clusterProfiler: an R package for comparing biological themes among gene clusters, OMICS 16 (2012) 284–287, https://doi.org/10.1089/omi.2011.0118.

[30] S. Hanzelmann, R. Castelo, J. Guinney, GSVA: gene set variation analysis for microarray and RNA-seq data, BMC Bioinf. 14 (2013) 7, https://doi.org/10.1186/1471-2105-14-7.

[31] D. Warde-Farley, S.L. Donaldson, O. Comes, K. Zuberi, R. Badrawi, P. Chao, M. Franz, C. Grouios, F. Kazi, C.T. Lopes, A. Maitland, S. Mostafavi, J. Montojo, Q. Shao, G. Wright, G.D. Bader, Q. Morris, The GeneMANIA prediction server: biological network integration for gene prioritization and predicting gene function, Nucleic Acids Res. 38 (2010) W214–W220, https://doi.org/10.1093/nar/gkq537.

[32] Z.P. Liu, C. Wu, H. Miao, H. Wu, RegNetwork: an integrated database of transcriptional and post-transcriptional regulatory networks in human and mouse, Database 2015 (2015), https://doi.org/10.1093/database/bav095 bav095.

[33] J. Xia, E.E. Gill, R.E. Hancock, NetworkAnalyst for statistical, visual and network-based meta-analysis of gene expression data, Nat. Protoc. 10 (2015) 823–844, https://doi.org/10.1038/nprot.2015.052.

[34] A.P. Davis, C.J. Grondin, R.J. Johnson, D. Sciaky, J. Wiegers, T.C. Wiegers, C.J. Mattingly, Comparative Toxicogenomics database (CTD): update 2021, Nucleic Acids Res. 49 (2021) D1138–D1143, https://doi.org/10.1093/nar/gkaa891.

[35] P. Shannon, A. Markiel, O. Ozier, N.S. Baliga, J.T. Wang, D. Ramage, N. Amin, B. Schwikowski, T. Ideker, Cytoscape: a software environment for integrated models of biomolecular interaction networks, Genome Res. 13 (2003) 2498–2504, https://doi.org/10.1101/gr.1239303.

[36] C.B. Steen, C.L. Liu, A.A. Alizadeh, A.M. Newman, Profiling cell type abundance and expression in bulk tissues with CIBERSORTx, Methods Mol. Biol. 2117 (2020) 135–157, https://doi.org/10.1007/978-1-0716-0301-7_7.

[37] Y. Wu, S. Yang, J. Ma, Z. Chen, G. Song, D. Rao, Y. Cheng, S. Huang, Y. Liu, S. Jiang, J. Liu, X. Huang, X. Wang, S. Qiu, J. Xu, R. Xi, F. Bai, J. Zhou, J. Fan, X. Zhang, Q. Gao, Spatiotemporal immune landscape of colorectal cancer liver metastasis at single-cell level, Cancer Discov. 12 (2022) 134–153, https://doi.org/10.1158/2159-8290.CD-21-0316.

[38] L. Li, Q. Huang, L. Yang, R. Zhang, L. Gao, X. Han, L. Ji, X. Zou, The association between non-alcoholic fatty liver disease (NAFLD) and advanced fibrosis with serological vitamin B12 markers: results from the NHANES 1999–2004, Nutrients 14 (2022) 1224. https://www.mdpi.com/2072-6643/14/6/1224.

[39] Z. Ruan, T. Lu, Y. Chen, M. Yuan, H. Yu, R. Liu, X. Xie, Association between psoriasis and nonalcoholic fatty liver disease among outpatient US adults, JAMA Dermatol 158 (2022) 745–753, https://doi.org/10.1001/jamadermatol.2022.1609.

[40] Z.M. Younossi, M. Stepanova, Y. Younossi, P. Golabi, A. Mishra, N. Rafiq, L. Henry, Epidemiology of chronic liver diseases in the USA in the past three decades, Gut 69 (2020) 564–568, https://doi.org/10.1136/gutjnl-2019-318813.

[41] Y. Huang, L. Wang, Y. Mao, G. Nan, Long noncoding RNA-H19 contributes to atherosclerosis and induces ischemic stroke via the upregulation of acid phosphatase 5, Front. Neurol. 10 (2019) 32, https://doi.org/10.3389/fneur.2019.00032.

[42] T. Morisawa, A. Nakagomi, K. Kohashi, Y. Kusama, W. Shimizu, Serum tartrate-resistant acid phosphatase-5b levels are associated with the severity and extent of coronary atherosclerosis in patients with coronary artery disease, J. Atherosclerosis Thromb. 24 (2017) 1058–1068, https://doi.org/10.5551/jat.39339.

[43] N. Oksala, M. Levula, M. Pelto-Huikko, L. Kytomaki, J.T. Soini, J. Salenius, M. Kahonen, P.J. Karhunen, R. Laaksonen, T. Parkkila, T. Lehtimaki, Carbonic anhydrases II and XII are up-regulated in osteoclast-like cells in advanced human atherosclerotic plaques-Tampere Vascular Study, Ann. Med. 42 (2010) 360–370, https://doi.org/10.3109/07853890.2010.486408.

[44] N. Graham, J.W. Pollard, An acid trip activates protumoral macrophages to promote hepatocellular carcinoma malignancy, J. Clin. Invest. 132 (2022), https://doi.org/10.1172/JCI158562.

[45] I. Ahrens, H. Domeij, S.U. Eisenhardt, D. Topcic, M. Albrecht, E. Leitner, K. Viitaniemi, J.B. Jowett, M. Lappas, C. Bode, I. Haviv, K. Peter, Opposing effects of monomeric and pentameric C-reactive protein on endothelial progenitor cells, Basic Res. Cardiol. 106 (2011) 879–895, https://doi.org/10.1007/s00395-011-0191-y.

[46] S. Shrivastava, E.G. Meissner, E. Funk, S. Poonia, V. Shokeen, A. Thakur, B. Poonia, S.K. Sarin, N. Trehanpati, S. Kottilil, Elevated hepatic lipid and interferon stimulated gene expression in HCV GT3 patients relative to non-alcoholic steatohepatitis, Hepatol Int 10 (2016) 937–946, https://doi.org/10.1007/s12072-016-9733-6.

[47] R.A. Saxton, D.M. Sabatini, mTOR signaling in growth, metabolism, and disease, Cell 168 (2017) 960–976, https://doi.org/10.1016/j.cell.2017.02.004.

[48] A. Lluch, S.R. Veiga, J. Latorre, J.M. Moreno-Navarrete, N. Bonifaci, V. Dien Nguyen, Y. Zhou, M. Horing, G. Liebisch, V.M. Olkkonen, D. Llobet-Navas, G. Thomas, R. Rodriguez-Barrueco, J.M. Fernandez-Real, S.C. Kozma, F.J. Ortega, A compound directed against S6K1 hampers fat mass expansion and mitigates diet-induced hepatosteatosis, JCI Insight 7 (2022), https://doi.org/10.1172/jci.insight.150461.

[49] J. Hou, J. Zhang, P. Cui, Y. Zhou, C. Liu, X. Wu, Y. Ji, S. Wang, B. Cheng, H. Ye, L. Shu, K. Zhang, D. Wang, J. Xu, Q. Shu, M. Colonna, X. Fang, TREM2 sustains macrophage-hepatocyte metabolic coordination in nonalcoholic fatty liver disease and sepsis, J. Clin. Invest. 131 (2021), https://doi.org/10.1172/JCI135197.

[50] E. Buzzetti, M. Pinzani, E.A. Tsochatzis, The multiple-hit pathogenesis of non-alcoholic fatty liver disease (NAFLD), Metabolism 65 (2016) 1038–1048, https://doi.org/10.1016/j.metabol.2015.12.012.

[51] S. Porte, E. Valencia, E.A. Yakovtseva, E. Borras, N. Shafqat, J.E. Debreczeny, A.C.W. Pike, U. Oppermann, J. Farres, I. Fita, X. Pares, Three-dimensional structure and enzymatic function of proapoptotic human p53-inducible quinone oxidoreductase PIG3, J. Biol. Chem. 284 (2009) 17194–17205, https://doi.org/10.1074/jbc.M109.001800.

[52] Q. Meng, X. Li, X. Xiong, Identification of hub genes associated with non-alcoholic steatohepatitis using integrated bioinformatics analysis, Front. Genet. 13 (2022) 872518, https://doi.org/10.3389/fgene.2022.872518.

[53] G.K. Hansson, A. Hermansson, The immune system in atherosclerosis, Nat. Immunol. 12 (2011) 204–212, https://doi.org/10.1038/ni.2001.

[54] Y. Cai, H. Li, M. Liu, Y. Pei, J. Zheng, J. Zhou, X. Luo, W. Huang, L. Ma, Q. Yang, S. Guo, X. Xiao, Q. Li, T. Zeng, F. Meng, H. Francis, S. Glaser, L. Chen, Y. Huo, G. Alpini, C. Wu, Disruption of adenosine 2A receptor exacerbates NAFLD through increasing inflammatory responses and SREBP1c activity, Hepatology (Baltimore, Md 68 (2018) 48–61, https://doi.org/10.1002/hep.29777.

[55] A. Remmerie, L. Martens, T. Thoné, A. Castoldi, R. Seurinck, B. Pavie, J. Roels, B. Vanneste, S. De Prijck, M. Vanhockerhout, M. Binte Abdul Latib, L. Devisscher, A. Hoorens, J. Bonnardel, N. Vandamme, A. Kremer, P. Borghgraef, H. Van Vlierberghe, S. Lippens, E. Pearce, Y. Saeys, C.L. Scott, Osteopontin expression identifies a subset of recruited macrophages distinct from kupffer cells in the fatty liver, Immunity 53 (2020), https://doi.org/10.1016/j.immuni.2020.08.004.

[56] X. Xiong, H. Kuang, S. Ansari, T. Liu, J. Gong, S. Wang, X.-Y. Zhao, Y. Ji, C. Li, L. Guo, L. Zhou, Z. Chen, P. Leon-Mimila, M.T. Chung, K. Kurabayashi, J. Opp, F. Campos-Pérez, H. Villamil-Ramírez, S. Canizales-Quinteros, R. Lyons, C.N. Lumeng, B. Zhou, L. Qi, A. Huertas-Vazquez, A.J. Lusis, X.Z.S. Xu, S. Li, Y. Yu, J. Z. Li, J.D. Lin, Landscape of intercellular crosstalk in healthy and NASH liver revealed by single-cell secretome gene analysis, Mol Cell 75 (2019), https://doi.org/10.1016/j.molcel.2019.07.028.

[57] P. Ramachandran, R. Dobie, J.R. Wilson-Kanamori, E.F. Dora, B.E.P. Henderson, N.T. Luu, J.R. Portman, K.P. Matchett, M. Brice, J.A. Marwick, R.S. Taylor, M. Efremova, R. Vento-Tormo, N.O. Carragher, T.J. Kendall, J.A. Fallowfield, E.M. Harrison, D.J. Mole, S.J. Wigmore, P.N. Newsome, C.J. Weston, J.P. Iredale, F. Tacke, J.W. Pollard, C.P. Ponting, J.C. Marioni, S.A. Teichmann, N.C. Henderson, Resolving the fibrotic niche of human liver cirrhosis at single-cell level, Nature 575 (2019) 512–518, https://doi.org/10.1038/s41586-019-1631-3.

[58] G.K. Hansson, Inflammation, atherosclerosis, and coronary artery disease, N. Engl. J. Med. 352 (2005) 1685–1695, https://doi.org/10.1056/NEJMra043430.

[59] F. Tacke, D. Alvarez, T.J. Kaplan, C. Jakubzick, R. Spanbroek, J. Llodra, A. Garin, J. Liu, M. Mack, N. van Rooijen, S.A. Lira, A.J. Habenicht, G.J. Randolph, Monocyte subsets differentially employ CCR2, CCR5, and CX3CR1 to accumulate within atherosclerotic plaques, J. Clin. Invest. 117 (2007) 185–194, https://doi.org/10.1172/JCI28549.

[60] F.K. Swirski, P. Libby, E. Aikawa, P. Alcaide, F.W. Luscinskas, R. Weissleder, M.J. Pittet, Ly-6Chi monocytes dominate hypercholesterolemia-associated monocytosis and give rise to macrophages in atheromata, J. Clin. Invest. 117 (2007) 195–205, https://doi.org/10.1172/JCI29950.

[61] J.E. Feig, J.X. Rong, R. Shamir, M. Sanson, Y. Vengrenyuk, J. Liu, K. Rayner, K. Moore, M. Garabedian, E.A. Fisher, HDL promotes rapid atherosclerosis regression in mice and alters inflammatory properties of plaque monocyte-derived cells, Proc Natl Acad Sci U S A 108 (2011) 7166–7171, https://doi.org/10.1073/pnas.1016086108.

[62] H. Jinnouchi, L. Guo, A. Sakamoto, S. Torii, Y. Sato, A. Cornelissen, S. Kuntz, K.H. Paek, R. Fernandez, D. Fuller, N. Gadhoke, D. Surve, M. Romero, F. D. Kolodgie, R. Virmani, A.V. Finn, Diversity of macrophage phenotypes and responses in atherosclerosis, Cell. Mol. Life Sci. 77 (2020) 1919–1932, https://doi.org/10.1007/s00018-019-03371-3.

[63] M. de Gaetano, D. Crean, M. Barry, O. Belton, M1- and M2-type macrophage responses are predictive of adverse outcomes in human atherosclerosis, Front. Immunol. 7 (2016) 275, https://doi.org/10.3389/fimmu.2016.00275.

[64] J. Gao, L. Shi, J. Gu, D. Zhang, W. Wang, X. Zhu, J. Liu, Difference of immune cell infiltration between stable and unstable carotid artery atherosclerosis, J. Cell Mol. Med. 25 (2021) 10973–10979, https://doi.org/10.1111/jcmm.17018.

[65] E. Dorochow, N. Kraus, N. Chenaux-Repond, S. Pierre, A. Kolbinger, G. Geisslinger, C. Ortiz, C. Welsch, J. Trebicka, R. Gurke, L. Hahnefeld, S. Klein, K. Scholich, Differential lipidomics, metabolomics and immunological analysis of alcoholic and non-alcoholic steatohepatitis in mice, Int. J. Mol. Sci. 24 (2023), https://doi.org/10.3390/ijms241210351.

[66] Y. Cao, W. Mai, R. Li, S. Deng, L. Li, Y. Zhou, Q. Qin, Y. Zhang, X. Zhou, M. Han, P. Liang, Y. Yan, Y. Hao, W. Xie, J. Yan, L. Zhu, Macrophages evoke autophagy of hepatic stellate cells to promote liver fibrosis in NAFLD mice via the PGE2/EP4 pathway, Cell. Mol. Life Sci. 79 (2022) 303, https://doi.org/10.1007/s00018-022-04319-w.

[67] X. Ficht, M. Iannacone, Immune surveillance of the liver by T cells, Sci Immunol 5 (2020), https://doi.org/10.1126/sciimmunol.aba2351.

[68] Z. Her, J.H.L. Tan, Y.S. Lim, S.Y. Tan, X.Y. Chan, W.W.S. Tan, M. Liu, K.S.M. Yong, F. Lai, E. Ceccarello, Z. Zheng, Y. Fan, K.T.E. Chang, L. Sun, S.C. Chang, C.L. Chin, G.H. Lee, Y.Y. Dan, Y.S. Chan, S.G. Lim, J.K.Y. Chan, K.G. Chandy, Q. Chen, CD4(+) T cells mediate the development of liver fibrosis in high fat diet-induced NAFLD in humanized mice, Front. Immunol. 11 (2020) 580968, https://doi.org/10.3389/fimmu.2020.580968.

[69] M. Ghazarian, X.S. Revelo, M.K. Nohr, H. Luck, K. Zeng, H. Lei, S. Tsai, S.A. Schroer, Y.J. Park, M.H.Y. Chng, L. Shen, J.A. D'Angelo, P. Horton, W.C. Chapman, D. Brockmeier, M. Woo, E.G. Engleman, O. Adeyi, N. Hirano, T. Jin, A.J. Gehring, S. Winer, D.A. Winer, Type I interferon responses drive intrahepatic T cells to promote metabolic syndrome, Sci Immunol 2 (2017), https://doi.org/10.1126/sciimmunol.aai7616.

[70] Y. Yang, Z. Huang, Z. Yang, Y. Qi, H. Shi, Y. Zhou, F. Wang, M. Yang, Serum metabolomic profiling reveals an increase in homocitrulline in Chinese patients with nonalcoholic fatty liver disease: a retrospective study, PeerJ 9 (2021) e11346, https://doi.org/10.7717/peerj.11346.

[71] S. Sutti, E. Albano, Adaptive immunity: an emerging player in the progression of NAFLD, Nature reviews, Gastroenterol. Hepatol. 17 (2020) 81–92, https://doi.org/10.1038/s41575-019-02102.

[72] Y. Tan, X. Liu, K. Zhou, X. He, C. Lu, B. He, X. Niu, C. Xiao, G. Xu, Z. Bian, X. Zu, G. Zhang, W. Zhang, A. Lu, The potential biomarkers to identify the development of steatosis in hyperuricemia, PLoS One 11 (2016) e0149043, https://doi.org/10.1371/journal.pone.0149043.

[73] Y. Deng, M. Pan, H. Nie, C. Zheng, K. Tang, Y. Zhang, Q. Yang, Lipidomic analysis of the protective effects of shenling baizhu san on non-alcoholic fatty liver disease in rats, Molecules 24 (2019) 3943, https://doi.org/10.3390/molecules24213943.

[74] X. Wu, M. Xu, M. Geng, S. Chen, P.J. Little, S. Xu, J. Weng, Targeting protein modifications in metabolic diseases: molecular mechanisms and targeted therapies, Signal Transduct. Targeted Ther. 8 (2023) 220, https://doi.org/10.1038/s41392-023-01439-y.